ISSN 1882-3440

TECHNOLOGY DEVELOPMENT CENTER NEWS

NATIONAL INSTITUTE OF INFORMATION AND COMMUNICATIONS TECHNOLOGY
Serial No. 26 September 2005

NiCT

CONTENTS

Technical Reports

Comparison of observed delays and delay rates between K4 and K5/VSSP system

Tetsuro Kondo (*kondo@nict.go.jp*)
and Yasuhiro Koyama

Kashima Space Research Center
Institute of Information and Communications Technology, 893-1 Hirai, Kashima, Ibaraki 314-8501, Japan

Abstract: Comparison of observed delays and delay rates between K4 and K5/VSSP system was carried out using JD0404 session data conducted on April 6, 2004. A chi-square evaluation shows that observed delays well coincide with each other, but suggests an existence of unmodeled error in observed delay rates when a period of scan length is less than 200 seconds.

1. Introduction

In order to evaluate the validity of correlation processing, it is a good idea to compare results obtained from independent correlation processing systems like a hardware correlator and a software correlator. Furthermore if signals are sampled by independent data acquisition terminals, it is possible to check the total validity of backend systems including a correlation processing. From this point of view, comparison of observed delays and delay rates between values obtained from K4 and K5/VSSP system has been carried out using the data of JD0404 session which was conducted on Apr. 6, 2004 as one of JADE (JApanese Dynamic Earth observation by VLBI) sessions coordinated by the Geographical Survey Institute (GSI).

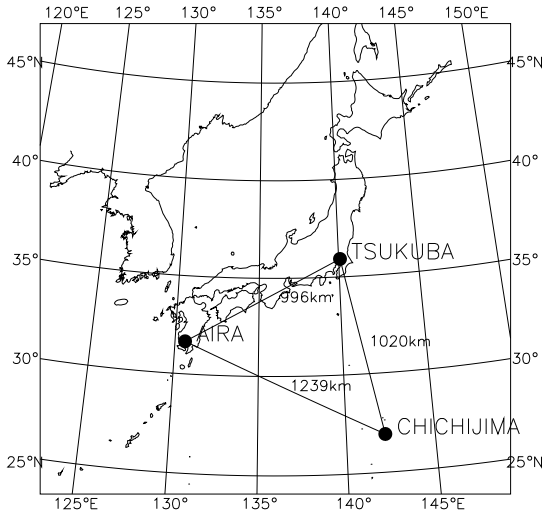

Figure 1. Location of main three stations participated in JD0404 session.

2. Data

2.1 Observation

Tsukuba (32m), Aira (10m), and Chichijima (10m) stations were participated in the JD0404 session (Fig.1).

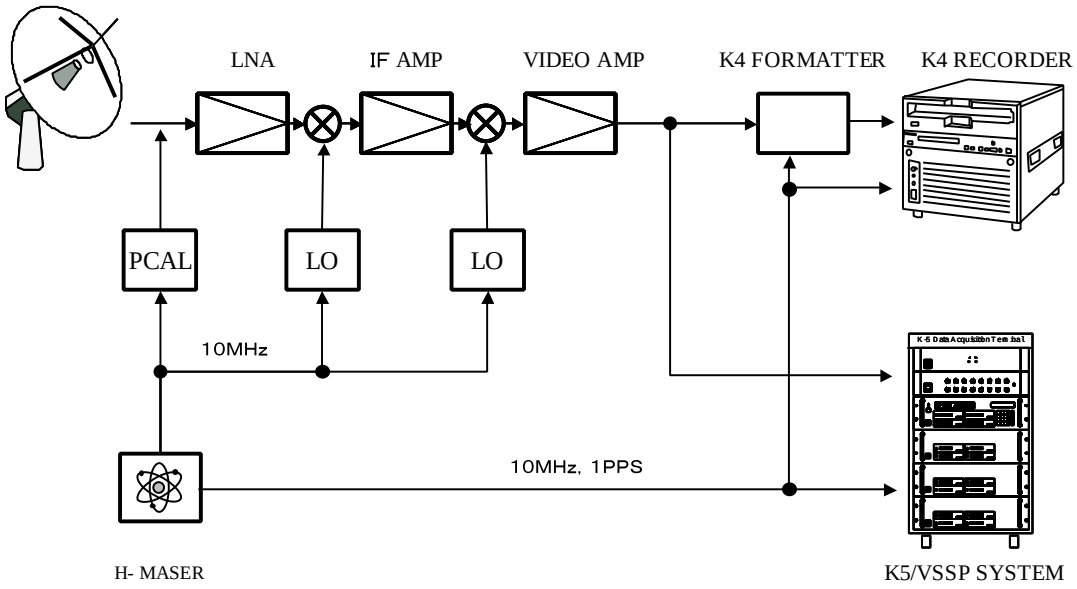

Figure 2: Block diagram of observation system.

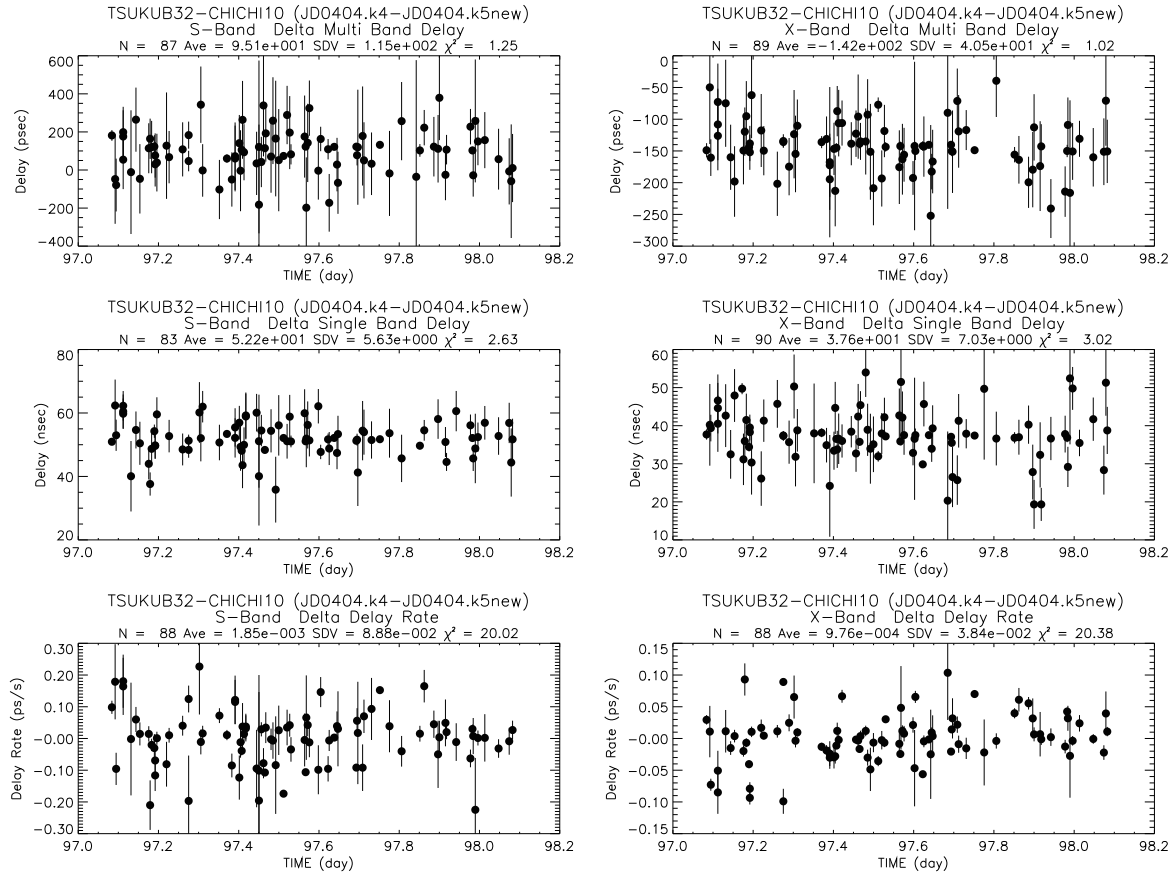

Figure 3. Results of comparison between K4 and K5/VSSP systems for Tsukuba-Chichijima. Left 3 panels are for S band data and right three panels are for X band data, and results of multi-band delay, single-band delay and delay rate are represented as function of time in top, middle and bottom panels, respectively.

Table 1. JD0404 session

Start time	02:00:00 UT (April 6, 2004)
End time	02:15:54 UT (April 7, 2004)
# of scans	239
Stations	Tsukuba (32m) Chichijima (10m) Aira (10m) Mizusawa (20m) Gifu (11m)
Observation mode	8 MHz, 1 bit sampling × 16 CH (X band : 8CH, S band: 8CH)

In this session a K4 recorder (16ch) and a K5/VSSP terminal consisting of four PCs (16ch) were operated simultaneously at three stations. Analog signal from the output of video converter was divided and fed to two systems (Fig.2). Table 1 summarizes the details of the session and the parameters of data sampling.

2.2 Correlation Processing

All correlation processings were performed at the GSI. K4 data were processed by using a KSP-type hardware correlator. K5/VSSP data were correlated by "cor" that is an XF type software correlator. The unit integration period at the correlation processing was 2 seconds and 1 second, respectively. Correlated data are further processed by "komb" that is a band-width synthesis program to obtain multi-band delay.

2.3 Comparison Condition

In a correlation processing we define reference time called PRT (Processing Reference Time) in a scan. A-priori values of delay and its time derivatives up to the third order are calculated at the PRT, so observed delay and delay rate are obtained

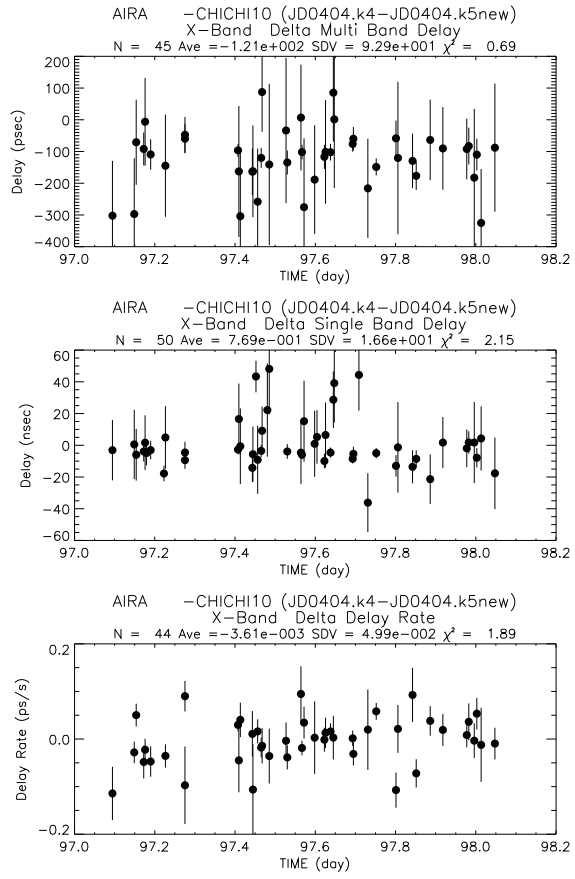

Figure 4. Results of Aira-Chichijima baseline with the same format as Fig.3 but for only X band data.

as those at the PRT. Therefore PRT should coincide with each other for the comparison of observed values between different systems. "Komb" capable of handling "cor" output data directly was developed to process K5/VSSP data.

PRT is usually taken at the center of a scan. PRT however can differ for every baseline when scan length differs for every baseline, and this will occur if schedule is made with a so-called subnet mode. JD0404 was scheduled under the subnet mode. K4 data were processed with PRT properly set for every baseline while K5/VSSP data were processed with PRT incidentally set same value for all baselines. As a result, more than half of the scans included in the session have different PRT between K4 data and K5/VSSP data. The discrepancy of PRT sometimes exceeds one minute, so that we use correlated data that have same PRT for both systems for a comparison study. In addition, we use the data that have the signal to noise ratio (SNR) of 7 or larger. Furthermore, we reject the data deviated more than 3σ from the average as an outlier in a statistical analysis.

Although K4 and K5/VSSP systems were operated at three stations, correlated data able to use for this study were limited to the Tsukuba-Chichijima baseline (S and X band data) and Aira-Chichijima baseline (X-band data only). Other correlated data were already deleted.

3. Results

Fig.3 represents the results of comparison for Tsukuba-Chichijima baseline. Left 3 panels are for S band data and right three panels are for X band data, and results of multi-band delay, single-band delay and delay rate are represented as function of time in top, middle and bottom panels, respectively. Ambiguities caused by the bandwidth synthesis are removed in the multi-band delays. Fig.4 shows the results of Aira-Chichijima baseline with the same format as Fig.3 but for only X band data. Table 2 summarizes the average, standard deviation, and χ^2 of differences. Here χ^2 is defined as

$$\chi^2 = \frac{1}{N-1}\sum_{n=1}^{N}\left(\frac{y(n)-\bar{y}}{\sigma y_{SNR}}\right)^2$$

where N is the number of data, $y(n)$ is the difference of observed values at the n-th data, $\bar{y}$ is the average of $y(n)$, and σy_{SNR} denotes the root sum square of 1σ error of each system computed from an SNR.

Existence of unmodeled error can be evaluated by χ^2, i.e., if it is larger than unity, the existence of unmodeled error source is sugestted. Chi square for multi-band delay are 1.25, 1.01, and 0.69 for Tsukuba-Chichijima S-band, Tsukuba-Chichijima X-band and Aira-Chichijima X-band, respectively. Hence the scatter of multi-band delays is well explained by an SNR error. However χ^2 for single-band delays is slightly larger than unity for all baselines and frequency bands. This suggests the existence of unmodeled error in single-band delay but it does not affect results so seriously. On the other hand, χ^2 for delay rates of Tsukuba- Chichijima baseline shows large number exceeding 20. To investigate a source of unmodeled error, data were sorted in three scan-length bins ($\leq$ 200, 200–300, $>$ 300 sec) and χ^2 was computed for each bin. Results are summarized in Table 3. It is clear from the table that large χ^2 is limited to the range of scan length $\leq$ 200 sec.

4. Conclusion

Comparison of observed delays and delay rates between K4 and K5/VSSP system was carried out in order to evaluate the validity of both systems

Table 2. Summary of comparison results

Tsukuba-Chichijima S-band	Average	Standard deviation	χ^2
multi-band delay	95.1 ps	114.8 ps	1.25
single-band delay	52.2 ns	5.6 ns	2.63
delay rate	0.002 ps/s	0.089 ps/s	20.02
Tsukuba-Chichijima X-band	**Average**	**Standard deviation**	χ^2
multi-band delay	-142.3 ps	40.5 ps	1.01
single-band delay	37.6 ns	7.0 ns	3.02
delay rate	0.001 ps/s	0.038 ps/s	20.38
Aira-Chichijima X-band	**Average**	**Standard deviation**	χ^2
multi-band delay	-120.7 ps	92.9 ps	0.69
single-band delay	0.8 ns	16.6 ns	2.15
delay rate	-0.004 ps/s	0.050 ps/s	1.89

Table 3. χ^2 of delay rate data of Tsukuba-Chichijima baseline for every scan-length bin

scan length (sec)	≤ 200	200–300	> 300
S-band	32.4	1.4	1.3
X-band	30.8	4.2	1.2

including correlation processing using JD0404 session data conducted on April 6, 2004. A chi-square evaluation shows that observed delays well coincide with each other, but it suggests an existence of unmodeled error in observed delay rates when a period of scan length is less than 200 seconds. This may explain the following fact that the inclusion of delay rate data in a KSP baseline analysis does not always give a good result. We are investigating the cause of this error.

Acknowledgments: The data used here were offered by Geophysical Survey Institute (GSI). We would like to thank K. Takashima of GSI for his kind permission of use of correlated data and J. Fujisaku of GSI for actual data transfer from GSI to NICT.

Timing Offset of the K5/VSSP System

Yasuhiro Koyama[1] (*koyama@nict.go.jp*),
Tetsuro Kondo[1], **Dan Smythe**[2],
Mike Titus[2], **and Alan Whitney**[2]

[1] *Kashima Space Research Center,*
National Institute of Information and
Communications Technology
893-1 Hirai, Kashima, Ibaraki 314-8501, Japan
[2] *Haystack Observatory,*
Massachusetts Institute of Technology,
Route 40, Westford, MA 01886, USA

Abstract: The timing offset of the K5/VSSP system relative to the Mark 5A system was measured by using a common noise signal recorded with the K5/VSSP system and the Mark 5A system at Haystack Observatory. The repeatability of the timing offset of the K5/VSSP system was also measured by comparing the different units of the K5/VSSP system. From these measurements, it was confirmed that the timing offset of the K5/VSSP with respect to the Mark 5A system is about 0.26 microseconds and the offset is stable and consistent to different sampling modes.

1. Introduction

In a geodetic VLBI measurement, the timing offset of the observing system at the reference station is indistinguishable with the UT1 – UTC estimate. It is therefore very important to know the systematic offset of the observing system and correct the offset in the data analysis procedure if there is any significant offset compared with the target accuracy of the UT1-UTC measurement. In 2002, the Working Group 2 of the IVS defined the target accuracy of the UT1 – UTC to be achieved by the year 2005 as 2 to 3 microseconds (Schuh, et al., 2002). To achieve this target accuracy, it is necessary to calibrate the offset among different geodetic VLBI sessions with a consistency better than 0.1 microsecond. However, it was reported that the systematic offset between the K3 formatter and the K5/VSSP system exists as large as 2.3 microsecond. The offset was found by processing a geodetic VLBI session data in which both K3 formatter and the K5/VSSP system were used in parallel at the Kashima 34m station. As this fact suggests, different observing systems may have different systematic timing offsets against each other reflecting the different designs of the A/D sampling mechanism and circuits. With this scope in mind, we performed measurements to determine the systematic offset of the K5/VSSP system with respect to the Mark 5A/Mark 4 back-end system and its stability within the K5/VSSP system. The methods and the results of the measurements will be presented in this report.

Figure 1. Set-up of the measurements.

2. Method of Measurements

To make the offset measurements, a common noise source was recorded with the K5/VSSP system and the Mark 5A system in parallel. A noise signal generated inside the Mark4 back-end terminal located at the "Tape Lab" room of the Haystack Observatory was used as the common signal. Mark 5A system recorded the data from the Mark4 formatter unit which is connected to the Mark4 baseband converters with usual signal route, whereas the K5/VSSP system sampled the analog baseband signal taken from the monitor connectors of the Mark4 baseband converter units. Set-up of the measurements is shown in the Figure 1 and Figure 2.

Only the four-channel configuration of the K5/VSSP system was used for the measurements. To ensure the timing of the 1-PPS (pulse per second) signals are identical to two units, a common 1-PPS signal was supplied to the Mark 5A system and the K5/VSSP system. The 1-PPS signal to the K5/VSSP unit was supplied by a coaxial cable with a length of 208 cm from the Mark 4 back-end system, and the length considered to be short enough since the timing delay caused by this cable is evaluated as about 4.2 nanosecond. Similarly, 10MHz reference signal for the K5/VSSP32 system was generated by using a signal generator with the 5MHz reference signal common with the Mark 5A system as the external reference signal. The data were recorded two times each on May 10, 2005 for three sampling modes, i.e. 4MHz,

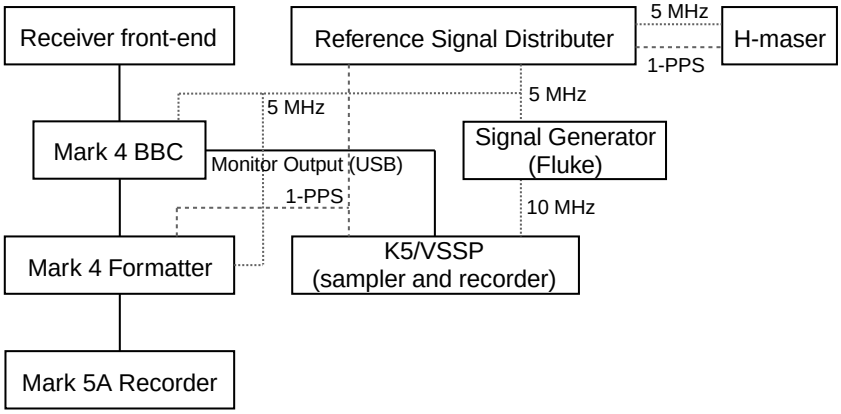

Figure 2. Schematic diagram of the signal route.

Table 1. Time delay recorded with the Mark 5A system with respect to the K5/VSSP system.

Sampling mode for each channel	Mark4 correlator (sec)	K5 software correlator (sec)
16MHz-1bit-16Mbps (1)	2.635×10^{-7}	2.621×10^{-7}
16MHz-1bit-16Mbps (2)	2.628×10^{-7}	2.621×10^{-7}
8MHz-1bit-8Mbps (1)	2.609×10^{-7}	2.616×10^{-7}
8MHz-1bit-8Mbps (2)	2.609×10^{-7}	2.616×10^{-7}
4MHz-1bit-4Mbps (1)	2.614×10^{-7}	2.640×10^{-7}
4MHz-1bit-4Mbps (2)	2.612×10^{-7}	2.636×10^{-7}

8MHz, and 16MHz. Only the 1-bit sampling modes were examined. After the data were recorded, the K5/VSSP32 data files were converted to the Mark 5A format files and then recorded into the disk-pack module of the Mark 5A system to correlate the data with the Mark 5A data by using Mark4 correlator system. In addition, the data recorded with the Mark 5A system were extracted and then converted to the K5/VSSP data file format files to correlate the data with the K5/VSSP data files by using the K5 software correlator system. In the cross correlation processing, the *a priori* parameters for the delay and delay rate were set to be zero to obtain systematic delay between the two observing systems.

3. Results

The offsets obtained from the correlation processing by using the Mark4 correlator and the K5 software correlator are shown in the Table 1. In the table, only the results for the 1st channel are shown. The positive value of the delay means the second station of the baseline receives the radio signal later than the first station. In the case of this measurements, the signal is common and the positive value of the delay means that the time tag written with the K5 system is behind to the Mark 5A system. Figure 3 shows the coarse delay functions for four different channels processed with the K5 software correlator.

To confirm that the systematic offset of the K5/VSSP system is constant, another test was performed on August 16, 2005 by using two independent units of the K5/VSSP system and recorded a common noise signal. The delay between two recorded data was calculated by using the K5 software correlator and the measurement was repeated by re-setting the sampler clock inside one of the K5/VSSP units. The upper-side-band signals from four baseband converters were supplied to the two K5/VSSP units by using T-connectors. Both 1-PPS signals and the 10MHz reference signals were supplied from an identical distributor unit. All the cables used in this measurement were same in length within a few centimeters. Therefore, we can assume the signal paths to the two K5/VSSP units are identical. Table 2 shows the results of this measurement. The sampling mode was 16MHz-1bit-16Mbps for each channel.

4. Conclusions

Considering the time interval of the data sampling is 6.25×10^{-8} second, all measured offsets between K5/VSSP units were smaller than the

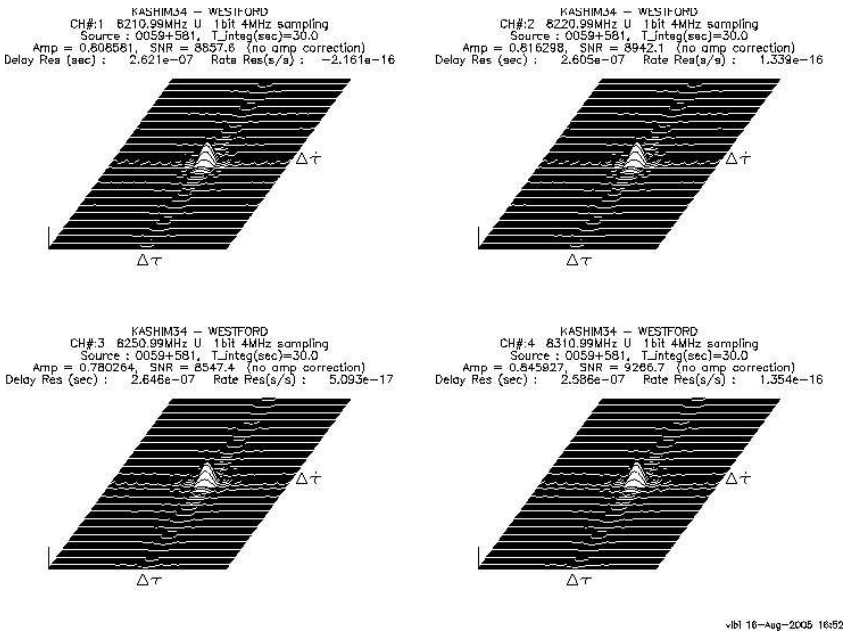

Figure 3. Coarse delay functions for four channels between Mark 5A data and K5/VSSP data.

Table 2. Time delay between recorded data using two K5/VSSP units.

Seq. No.	Ch. 1 (sec)	Ch. 2 (sec)	Ch. 3 (sec)	Ch. 4 (sec)
1	4.325×10^{-8}	1.798×10^{-8}	2.045×10^{-8}	0.127×10^{-8}
2	4.343×10^{-8}	1.656×10^{-8}	1.918×10^{-8}	0.135×10^{-8}
3	4.344×10^{-8}	1.509×10^{-8}	1.742×10^{-8}	0.135×10^{-8}
4	4.355×10^{-8}	1.373×10^{-8}	1.543×10^{-8}	0.136×10^{-8}
5	4.360×10^{-8}	1.259×10^{-8}	1.356×10^{-8}	0.133×10^{-8}

sampling interval. Since our target accuracy of the UT1 – UTC is 2 to 3 microsecond and we need to calibrate the systematic offset of the observing system to the level of 0.1 microsecond, the variation of the offset shown in the Table 2 is considered to be negligible. The results shown in the Table 1 suggest that the K5/VSSP system has a constant delay of about 0.26 microsecond with respect to the Mark 5A/Mark 4 back-end system. This value should be used to correct the systematic offset of the K5/VSSP system when the reference station in the correlation processing used the system. This value is also applicable if the A/D sampling is done with the same configuration, for example the Mark 4 recorder is used with the Mark 4 back-end system. However, if the A/D sampling is done with the other systems, i.e. VLBA formatter for example, different offset have to be used. Moreover, only the relative offsets between different observing systems were discussed in this report. To improve the absolute accuracy of the UT1 – UTC, it is necessary to evaluate the absolute offsets of the observing systems and this problem should be tackled as the next step of the investigations in the future.

References

Schuh, H., C. Patrick, H. Hase, E. Himwich, K. Kingham, C. Klatt, C. Ma, Z. Malkin, A. Niell, A. Nothnagel, W. Schlüter, K. Takashima, and N. Vandenberg (2002), Final Report, IVS Working Group 2 for Product Specification and Observing Program, in International VLBI Service for Geodesy and Astrometry-2001 Annual Report, by N. Vandenberg and K. Baver (eds.), NASA/TP-2002-00817-0, pp. 13-45.

Himwich, E (2005), Network Coordinator Report, in International VLBI Service for Geodesy and Astrometry-2004 Annual Report, by D. Behrend and K. Baver (eds.), NASA/TP-2005-212772, pp. 31-37.

Multi-channel Gbps Geodetic VLBI Experiment

Yasuhiro Koyama (*koyama@nict.go.jp*), **Tetsuro Kondo, Moritaka Kimura, and Hiroshi Takeuchi**

Kashima Space Research Center,
National Institute of Information and Communications Technology
893-1 Hirai, Kashima, Ibaraki 314-8501, Japan

Abstract: A multi-channel Gbps geodetic VLBI experiment was performed for the first time with the single baseline between Kashima 11m and Koganei 11m VLBI stations. At each station, both X-band and S-band signals were recorded with the K5 VLBI system at the total data rate of 1024Mbps by assigning 10 channels and 6 channels to the X-band and S-band, respectively. The data were then processed with the K5 software correlator and the results were analyzed to evaluate the performance of the observing system. The preliminary results of this experiment will be reported.

1. Introduction

In the geodetic VLBI measurements, the accuracy and precision of the estimated parameters such as coordinates of the reference points of the radio telescopes or the Earth Orientation Parameters (EOP) are affected by the number of available scans in a measurement session and the individual precision of delay observable of each scan. To increase the number of scans in a session with a given set of radio telescopes, it is necessary to improve the sensitivity of the observing system by increasing the total data rate of the observations. Since the signal to noise ratio is proportional to the square root of the total bandwidth of the observations, it is possible to decrease the integration time by using higher sampling rate without decreasing the signal to noise ratio for each scan. In the case of small aperture radio telescopes with relatively fast slewing rate like 11-m VLBI stations at Kashima and Koganei, the effect is considered to be very large. Attempts to increase the total data rate to Gbps class was initiated in 1998 by using the high speed digital oscilloscope (Tektronics TDS784/TDS580) as the single-channel AD sampler unit at the sampling rate of 1024Mbps (Koyama, et al., 2000). The interface unit DD-1 was designed to interface with the Gbps data recorder unit (Toshiba GBR1000). The first geodetic VLBI experiment was performed for about 6 hours on October 19, 1999 with the 11m VLBI stations at Kashima and Koganei. The recorded data were processed with the GICO correlator which was modified from the Ultra Wide-band Correlator originally developed for the Nobeyama Millimeter Array of the Nobeyama Radio Observatory. After a series of geodetic VLBI experiments were performed with the initial developments of the Gbps VLBI system, the single-channel VLBI sampler unit ADS1000, the Gbps recorder unit GBR2000, and the correlator system GICO2 were developed (Takeuchi, et al., 2003). At this stage, all the components, i.e. ADS1000, GBR2000, and GICO2, were designed to be VSI-H compliant and the system was used to evaluate geodetic VLBI at the Gbps class of total data rate. The ADS1000 is capable to sample single channel base-band signal at the sampling rate of 1024MHz. The sampling bits can be selected from either one bit or two bits. The unit is equipped with the two VSI-H connector ports to support 2048Mbps maximum total data rate with the 32MHz data clock which is defined as basic specification of the VSI-H. A series of geodetic VLBI experiments were then performed and it was confirmed that the Gbps VLBI system can perform better than the K4 VLBI system which is operational up to 256Mbps total data rate.

On the other hand, the individual precision of delay observable of each scan is determined by the effective bandwidth defined as the standard deviation of the observation frequencies of all channels in a receiving band in the case of multi-channel observing system. In this sense, the multi-channel observing system has a great advantage compared with the single-channel observing system because bandwidth synthesis technique can expand the effective bandwidth of the observations. The multi-channel system is also usually better than the single-channel system because it is possible to compensate for the phase delay characteristic over the receiving bands by using phase calibration signal. Inability to perform ionospheric delay correction was also one of the disadvantage of the single-channel observing system, but this problem can also be solved by using the multi-channel observing system. With these scopes in mind, a multi-channel Gbps sampler unit, named ADS2000, has been developed as one of the component of the K5 VLBI system. A test geodetic VLBI experiment was performed on March 11, 2005 by using the ADS2000 sampler unit and the K5 VLBI recording system. The data were then processed with the K5 software correlator. The detail of the experiment and its preliminary results will be reported in the remaining of this report.

Figure 1. ADS2000 16-channel 2Gbps VLBI sampler unit.

2. Observing System

As one of the components of the K5 VLBI system, the multi-channel 2Gbps A/D sampler unit ADS2000 has been developed. The picture of the unit is shown in the Figure 1. The unit is capable to sample baseband signals up to 16 channels. The sampling rate and bits for each channel are fixed to 64MHz and 2 bits, respectively. The unit is equipped with two interface connectors which are compliant with the VSI-H specifications. Basic specifications of the VSI-H defined with the 32MHz data clock is supported by using 2 interface ports, where as the optional specifications of the VSI-H defined with the 64MHz data clock is supported by using one of the two interface ports. In the latter case, the 32 data streams are assigned to either upper or lower bits of the 2bits sampling data. In the case of 32MHz data clock, lower bits are assigned to the primary VSI-H output port, and the upper bits are assigned to the secondary VSI-H output port.

The data streams from the VSI-H output ports of the ADS2000 are then recorded to the internal hard disk system of the K5 recording system by using a PC-VSI board on PCI (Peripheral Component Interconnect) bus of the system. RAID (Redundant Arrays of Inexpensive Disks) is configured to support high speed data recording to the hard disk system. Currently, data rate of 1024Mbps can be supported by using single PC system as a K5 recording system, and efforts to support 2048Mbps data stream is continuing. It was confirmed that the PC-VSI board can support 64MHz data clock mode to support 2048Mbps data rate, but the recording speed to the internal hard disk units is not fast enough to support the 2048Mbps recording.

Figure 2. A set of the K5 VLBI system used at Koganei 11m VLBI station.

3. Experiments

The experiment was performed for 24 hours from 03:00 UT on March 11, 2005. Two 11-m VLBI stations at Kashima and Koganei were used for the observations. At each station, ADS2000 sampler unit was connected to the USB (Upper Side Band) output connectors of the K4 baseband converter units. Since the baseband converter units are not equipped with the 16MHz low pass filters, 32MHz low pass filters inside the units were used and external 16MHz low pass filters were used in addition by inserting the filters between the baseband converter output and the ADS2000 unit. The sampled data were recorded by using K5 recording units equipped with the PC-VSI board on the PCI bus. For this particular experiment, eight Serial ATA hard disk drives were configured as RAID-0. One of the two VSI-H output connectors on the ADS2000 unit was used and the data were generated with the 64MHz data clock. On the K5 recording system, every other data bits are skipped to effectively record 32MHz sampling data. 2 bits of data were recorded for each 16 channel data streams and then the total recorded data rate was 1024Mbps. Figure 2 shows the ADS2000 unit and the K5 recording system used at the Koganei site. The ADS2000 unit can be seen on the 19-inch rack and

the recording system can be seen on the right of the rack. The rack is the K5/VSSP (Versatile Scientific Sampling Processor) system and was not used for the experiment, this time. The baseband converter units can be seen behind the rack. The units are the same ones which were used during the Key Stone Project conducted from 1994 through 2001 (Koyama, et al., 1997). The frequency sequence of the 16 observing] channels were also chosen identical to the Key Stone Project.

In the 24 hour VLBI experiment session, 1722 observation scans were scheduled. At both stations, no scans were lost and all the observation scans were recorded with the K5 recording systems. Integration time for each scan was calculated to ensure signal to noise ratio of 20 and minimum length of scan of 10 seconds. The data recorded at Koganei site were transferred to Kashima after the session by using the high speed network connection between these sites. Each data file was then divided into 16 files which contains recorded data for each channel with the K5 data file format. For the correlation processing, the program **fx_cor** was used. The **fx_cor** is an FX type software correlator program and can handle 2-bits sampling data as in this case. To accelerate the processing speed, 10 CPUs were used for distributed processing in parallel. After the correlation processing, Mark3 database files were generated both for S-band and X-band and the data were analyzed to estimate various parameters such as coordinates of the Koganei 11-m station, clock offsets, and atmospheric delay parameters. The coordinates of the Kashima 11-m station was fixed to the ITRF2000 coordinates and the Earth Orientation Parameters were obtained from the IERS Bulletin B. SOLVE and CALC geodetic VLBI data analysis programs developed at the Goddard Space Flight Center of NASA were used to analyze the data.

4. Results

Figure 3 and 4 shows the distribution of the residual delay after the parameter fitting. Figure 3 shows only the valid data points with some deleted points due to the low signal to noise ratio. On the other hand, the Figure 4 shows all of the obtained delay no matter whether the data are used or not. The data points with large delay residual were removed from the data analysis and indicated by the small alphabet letters. As seen in the Figure 4, a lot of data were removed and these are a few blocks with similar delay residual at about 20, -13, and -26 nanoseconds. The reason of this split is still unknown. Also, many data points were removed from the data analysis due to the low signal to noise ratio. It seems the calculation of the signal

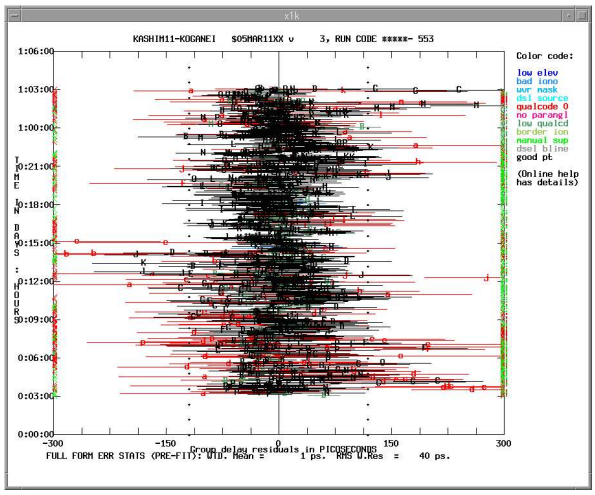

Figure 3. Residual delay after the parameter fitting. The vertical axis is the time in the session and the horizontal axis is the residual delay in the unit of second. Internal uncertainties of the delay is indicated by the horizontal error bar.

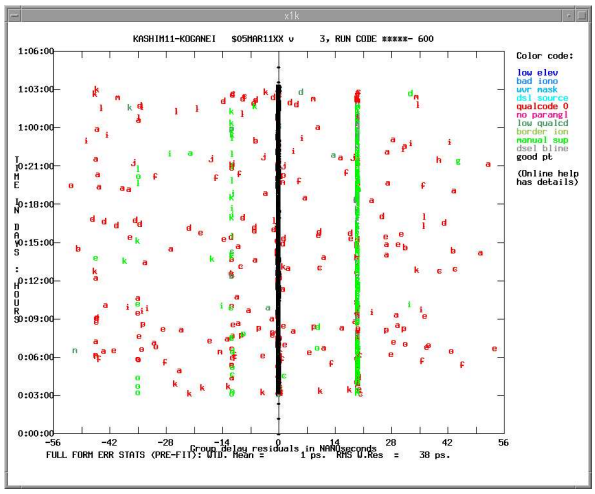

Figure 4. Residual delay after the parameter fitting with extended window for the horizontal axis. The vertical axis is the time in the session and the horizontal axis is the residual delay in the unit of second. Internal uncertainties of the delay is indicated by the horizontal error bar.

to noise ratio when the schedule file was generated was wrong and integration time was not enough for many observation scans.
The RMS of the residual delay was about 40 psec and this value is comparable to the typical RMS delay for the Key Stone Project which was about 30 to 40 psec. The uncertainty of the baseline length between Kashima 11m and Koganei 11m stations was evaluated as 1.34 mm and is also comparable or better than the typical Key Stone Project results with the K4 VLBI system performed with the total data rate of 256Mbps per site.

5. Conclusions and Future Plans

The multi-channel 2Gbps sampler unit ADS2000 has been developed and was used for the actual geodetic VLBI experiment for the first time at the data rate of 1024Mbps per site. Preliminary results indicated that the performance of the system is basically fine. It was also demonstrated that the K5 VLBI system can be configured to adopt itself for the multi-channel giga-bit Geodetic VLBI observations. It is expected that the K5 VLBI system can support up to 2048Mbps data rate per site by improving the recording speed limit to the internal hard disk raid system inside the K5 recording system. We would like to repeat the similar experiments with the ADS2000 system so that we can evaluate the performance of the unit as well as the overall performance of the K5 system in total.

References

Koyama, Y., T. Kondo, J. Nakajima, M. Sekido, R. Ichikawa, E. Kawai, H. Okubo, H. Osaki, H. Takaba, M. Yoshida, and K. Wakamatsu (2000), Geodetic VLBI Observations using the Giga-bit VLBI System, in International VLBI Service for Geodesy and Astrometry 2004 General Meeting Proceedings, eds. N. R. Vandenberg and K. D. Baver, NASA/CP-2004-212255, pp. 98-102

Koyama, Y., R. Ichikawa, T. Gotoh, M. Sekido, T. Kondo, N. Kurihara, F. Takahashi, J. Amagai, T. Otsubo, H. Nojiri, K. Sebata, H. Kunimori, H. Kiuchi, A. Kaneko, Y. Takahashi, S. Hama, Y. Hanado, M. Imae, C. Miki, M. Hosokawa, and T. Yoshino (1997), VLBI, SLR, and GPS observations in the Key Stone Project, Proceedings of the IAG Scientific Assembly, Geodesy on the Move, Gravity, Geoid, Geodynamics, and Antarctica (September 3-9, 1997, Rio de Janeiro), IAG Symposia Vol.119, pp. 394-399.

Takeuchi, H., J. Nakajima, M. Kimura, Y. Koyama, and T. Kondo (2003), Geodetic VLBI Experiments Using VSI-based Giga-bit VLBI System, IVS CRL-TDC News, No. 23, pp. 23-25.

Development of the new VLBI facility with a 2.4-m dish antenna at NICT

ICHIKAWA Ryuichi (*richi@nict.go.jp*), **KUBOKI Hiromitsu, KOYAMA Yasuhiro, NAKAJIMA Junichi, and KONDO Tetsuro**

Kashima Space Research Center
Institute of Information and Communications Technology, 893-1 Hirai, Kashima, Ibaraki 314-8501, Japan

We can almost realize to perform real-time or quasi-real-time VLBI observations such as the monitoring of the earth orientation and the precise positioning of interplanetary spacecraft using the recent e-VLBI technology. Our "K5 VLBI system" of the NICT is one of the e-VLBI technology which includes the multiple PC-based VLBI system and the original software packages including data sampling and acquisition, real-time IP data transmission, and correlation analysis. In addition, even if a small dish antenna is used, wide bandwidth Gigabit AD samplers such as ADS1000 and ADS2000[1] also enable to perform VLBI observations with high sensitivity.

To improve the VLBI station coverage (for example, the Pacific and southern hemisphere) such a compact VLBI system is very useful. Therefore, we are developing a compact VLBI facility with a 2.4 m diameter dish antenna. We consider this facility as an extended version of the CARAVAN (Compact Antenna of Radio Astronomy for VLBI Adapted Network) which is dedicated to network experiment before telescope time allocated to large dish[2]. So, we call this 'CARAVAN2400' hereafter. The CARAVAN2400 is shown in Figure 1. The 8 GHz low noise amplifier is installed behind the 2.4-m diameter dish and it is operated in normal temperature. The down converter including a reference frequency supply is assembled in the steel container and the container is attached on the side of the antenna pillar. The CARAVAN2400 can be operated at the 1.0 degree per second maximum tracking speed for both azimuth and elevation angles.

On 30 March 2005, we successfully captured the X-band solar signal using the CARAVAN2400, achieving "first light". We are now investigating receiver and system noise temperature in order to evaluate the performance of the system. After the system evaluation we are going to perform a first VLBI experiment with the Kashima 34-m antenna as of the end of this year. At the next step, we have a plan of the VLBI experiments using K5/PC-VSI Gigabit system to establish a high sensitive VLBI system. Our final goal is to utilize the CARAVAN2400 for the earth orientation monitoring and the spacecraft tracking.

Figure 1. The CARAVAN2400 at Kashima. The 34-m antenna is also shown behind the CARAVAN2400.

References

[1] Kimura, M., J. Nakajima, H. Takeuchi, and T. Kondo, 2-Gbps PC architecture and Gbps data processing in K5/PCVSI, *IVS CRL-TDC News*, No.23, pp.12-13, Nov. 2003.

[2] Yonezawa, I., Nakajima, J., Ohkubo, H., Tsuboi, M., and Kasuga, T., Development of compact VLBI system, *CRL IVS TDC news*, No.21, pp.29-30, 2002.

An evaluation of atmospheric path delay correction in differential VLBI experiments for spacecraft tracking

ICHIKAWA Ryuichi (*richi@nict.go.jp*),
SEKIDO Mamoru,
TAKEUCHI Hiroshi,
KOYAMA Yasuhiro,
KONDO Tetsuro,

Kashima Space Research Center, National Institute of Information and Communications Technology, 893-1 Hirai, Kashima, Ibaraki 314-8501, Japan

MOCHIDUKI Nanako,
MURATA Yasuhiro,
YOSHIKAWA Makoto,

Institute of Space and Astronautical Science Japan Aerospace Exploration Agency

OHNISHI Takafumi,

Space Solutions Department, Advanced Science Solutions Group, Fujitsu Limited

and Spacecraft DVLBI group

GSI, NAO, Hokkaido Univ., Gifu Univ., and Yamaguchi Univ.

Abstract: We evaluate an effect of cancelling out atmospheric path delay errors on differential VLBI measurements for the HAYABUSA spacecraft based on the delays derived from geodetic GPS analysis. The experiments were carried out on October 16 and 18, 2004. A large difference value of up to 10 cm of the differential path delay for the Kashima-Uchinoura baseline was estimated during the second experiment period. It is considered that this large value is caused by the high water vapor content due to the typhoon approaching at Uchinoura, the constellation of the baseline vector and difference in elevation angle at two stations.

1. Introduction

We performed differential VLBI ($\Delta VLBI$) experiments for tracking of the interplanetary spacecraft. Our main goal is to obtain the precise and quasi-realtime navigation technique of the spacecraft using $\Delta VLBI$ technique. With VLBI time delay measurements, differenced between the spacecraft and angularly nearby quasars to cancel common measurement errors such as the propagation delays due to the ionosphere and the neutral atmosphere. However, we can't always observe desirable quasars. It is possible that they have no enough intensity of the source flux to detect fringes. Unfortunately, sometimes we have no choice but to use quasars which are angularly far from the spacecraft. Then, we tried to evaluate the effects cancel by subtracting the group delays of the reference radio source from those of the spacecraft. In this short report, we focus on the issue of the path delay due to the neutral atmosphere estimated by geodetic GPS measurements.

2. VLBI and GPS measurements

Two HAYABUSA $\Delta VLBI$ experiments were carried out in order to evaluate reducing propagation delays due to the ionosphere and neutral atmosphere using $\Delta VLBI$ technique on October, 2004. The spacecraft HAYABUSA, which means "Falcon" in Japanese, was launched on May 9 2003, and has been flying steadily towards an asteroid named "Itokawa", after the late Dr. Hideo Itokawa, the father of Japan's space development program. It will orbit the asteroid as of September 2005, land on it, and bring back a sample from its surface.
The experiment IDs of October 16th and 18th are "hy4290" and "hy4292", respectively. We use Kashima 34-m, Kashima 11-m and Koganei-11m of NICT, Usuda 64-m and Uchinoura 34-m of ISAS/JAXA, and Tsukuba 32-m of GSI antennas for the experiments at X-band. The VLBI stations in this study are shown in Figure 1. We acquire the VLBI data using K5/VSSP system developed by National Institute of Information and Communications Technology (NICT).
The observing time for each day was scheduled during 0700 to 1400UT. We actually shorten it from 7 hours to less than 4 hours adjusting to the operation schedule of the spacecraft on October 16th. However, we unavoidably interrupt the second experiment around 0600UTC on October 18th due to the typhoon approaching.
The HAYABUSA spacecraft and an angularly nearby quasar "2126-158" were observed sequentially, not simultaneously, during each period with various time intervals of data acquisition (i.e. 50 seconds, 110 seconds, and 170 seconds). These switching intervals are chose in order to investigate an effect on the phase delay analysis. A result of the investigation will be described in the another report. Two quasars, "NRAO530" and "3C454.3", were also observed at the beginning and the end of the experiment period as a reference source for determining a clock offset. Figure 2 is an example of source trajectories on 18th October 2004 at

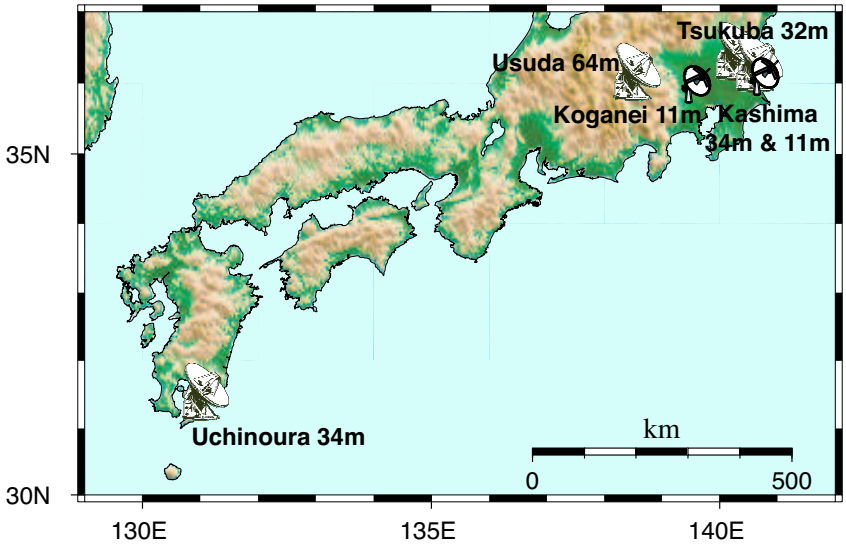

Figure 1. VLBI stations participated HAYABUSA DVLBI experiments

Table 1. Geodetic GPS stations nearby VLBI stations

VLBI station name	corresponding GPS station ID	Agency
Kashima 34-m and 11-m	KSMV (IGS)	KSRC, NICT
Koganei 11-m	KGNI (IGS)	NICT
Tsukuba 32-m	TSKB (IGS)	GSI
Usuda 64m	USUD (IGS)	ISAS/JAXA
Uchinoura 34-m	940099 (GEONET of GSI)	ISAS/JAXA

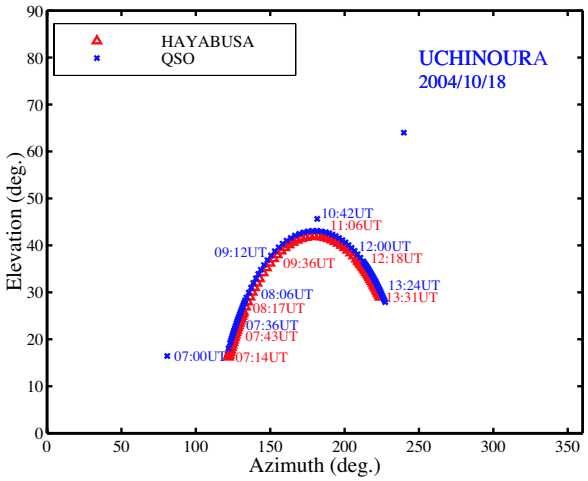

Figure 2. Source positions on 18 October 2004 at Uchinoura

Uchinoura. The maximum angular separations of the spacecraft from the quasar "2126-158" are less than 3 degrees.

In addition, we also acquire the data sets of the corresponding GPS stations nearby the each VLBI station (Table 1). The GPS station "940099" is one of the GPS Earth Observation Network (GEONET), Geographical Survey Institute (GSI) in Japan and it is located at about 1 km north-east from Uchinoura 34-m antenna. Other GPS stations are registered with the International GPS Service for Geodynamics (IGS)[1] and all of them are adjacent to each VLBI antenna. These GPS stations are continuously operated and the various data sets including raw data, precise orbit, satellite clock, earth orientation parameters and so on are archived in the anonymous ftp servers(ex. [2], [3]).

3. Meteorological condition

Figure 3 shows synoptic weather charts around Japan from 0000UTC of 16th to 0000UTC of 19th October 2004. During the first experiment

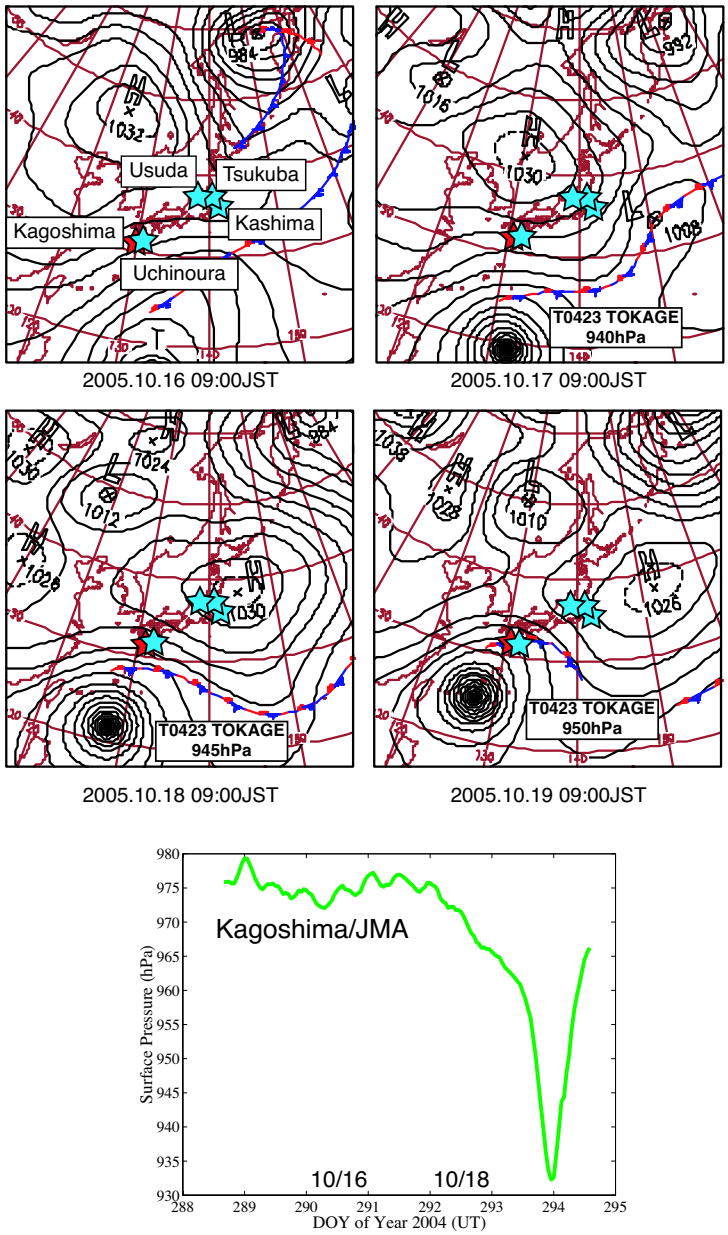

Figure 3. Upper: Synoptic weather charts around Japan from 0000UTC of 16th to 0000UTC of 19th October, 2004. Dark gray star and bright gray stars indicate the location of Kagoshima meteorological observatory, Japan Meteorological Agency (JMA) and the VLBI stations, respectively; Lower: Surface pressure change during 14-20 October, 2004 at Kogoshima meteorological observatory of JMA.

(hy4290), it was sunny and calm weather around Japan islands. After the 17th October, the strong typhoon 0423 (TOKAGE) was approaching south of Kyushu island, where Uchinoura station is located. The significant pressure depression at Kagoshima meteorological observatory of Japan Meteorological Agency (JMA), which is located about 100 km west of Uchinoura, is indicated in Figure 3 (lower panel). So, we unfortunately have to interrupt the hy4292 experiment around 0900UTC. The typhoon center was passed about 100 km east of Uchinoura on 20th October and it hit the central Japan with severe damage caused by heavy rainfall and strong wind.

4. Estimation of atmospheric delay by GPS measurements

4.1 Zenith wet delay

First, we estimate path delay due to the neutral atmosphere at zenith direction (ZTD: Zenith Total Delay) for each station through the double-difference procedure using the Bernese GPS software version 4.2[4]. Next, we calculate the zenith path delay due to the water vapor (ZWD: Zenith Wet Delay) by subtracting the zenith hydrostatic delay (ZHD: Zenith Hydrostatic Delay) from the ZTD. The ZHD which is mainly caused by the dry components of the atmosphere is determined by surface pressure measurements[5].

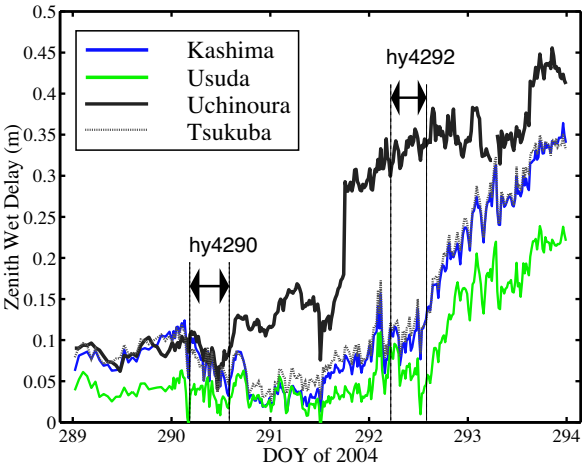

Figure 4. ZWD time series derived from GPS data sets at Kashima, Tsukuba, Usuda, and Uchinoura.

Time series of ZWD values at Kashima, Tsukuba, Usuda, and Uchinoura during 15 to 19 October 2004 are shown in Figure 4. On October 16th, which is the day of the hy4290 experiment, the ZWD values at all stations are less than 10 cm and it is consistent with the calm weather as shown in Figure 3. The ZWD value at Uchinoura dramatically increased from 15 cm to 27 cm within one hour on October 17th with the approach of typhoon TOKAGE. The ZWD values at Kashima and Tsukuba gradually increased up to 35 cm after October 18. At Usuda, where station altitude is above 1500 m, the ZWD value is relatively small compared with the values at other stations because of a low water vapor content at high altitude. However, even at Usuda the ZWD value was up to 25 cm until the end of October 19th. As shown in Figure 3 and 4, since meteorological conditions were significantly different between two experiment periods, we consider that those experiments are very suitable for our study.

4.2 Slant delay and differential delay

Conventionally, the slant-path wet delay ΔSLW_i at i_{th} epoch can be computed from the ZWD via

$$\Delta SLW_i = NMF(\theta_i) \times ZWD_i \qquad (1)$$

where $NMF(\theta_i)$ is the Niell mapping function[6] and θ_i is an elevation angle of the HAYABUSA spacecraft or nearby quasar at i_{th} epoch. Next, we calculate resampled slant-path wet delay values $\Delta SLW'$ over the whole experiment period for each station using piecewise cubic spline interpolation. A principle observable feature of VLBI is the difference in arrival times of radio signals between two stations. Then, we calculate differences between the values $\Delta SLW'$ at each station. We define this "differential wet delay". The differential wet delay for the HAYABUSA spacecraft is shown by:

$$D\Delta SLW^H_{AB}{}' = \Delta SLW^H_A{}' - \Delta SLW^H_B{}' \qquad (2)$$

where $D\Delta SLW^H_{AB}{}'$ is the differential wet delay for the baseline vector between the stations A and B and superscripts H denotes the HAYABUSA spacecraft. In the same way, the differential wet delay for the quasar $D\Delta SLW^Q_{AB}{}'$ is also shown by:

$$D\Delta SLW^Q_{AB}{}' = \Delta SLW^Q_A{}' - \Delta SLW^Q_B{}' \qquad (3)$$

where superscripts Q denotes the quasar. Figure 5 is an example of time series of the differential wet delay during the first experiment period (hy4290). Finally we calculate differences between both differential wet delays of the HAYABUSA spacecraft and those of the quasar:

$$D\Delta SLW^{QH}_{AB}{}' = D\Delta SLW^Q_{AB}{}' - D\Delta SLW^H_{AB}{}' \qquad (4)$$

where $D\Delta SLW^{QH}_{AB}{}'$ denotes the difference between two differential delays. If the angular separation is sufficiently small, the differential wet delays for both radio sources are almost equal. Then, these are canceled out by the difference procedures written in the equation (4). However, if these are different, the differences between them is added directly to the observables as an error source.

5. Results

Figure 6 shows time series of difference values, which are mentioned in the previous section (equation (4)), between two differential delays during the hy4290 experiment (a) and the hy4292 experiment (b).

The ZWD time series at all stations as shown in Figure 4 are consistent well each other in both amplitude and phase through the first experiment period. Thus, the differences values are almost equal

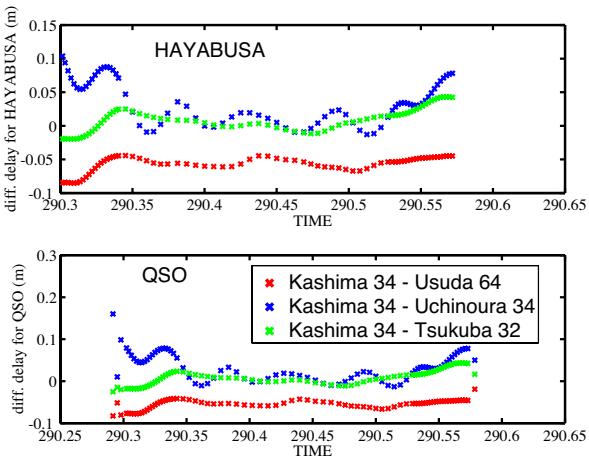

Figure 5. Upper: Differential wet delay for the HAYABUSA spacecraft during the hy4290 experiment on 16 October 2004; Lower: Same plot but for the quasar.

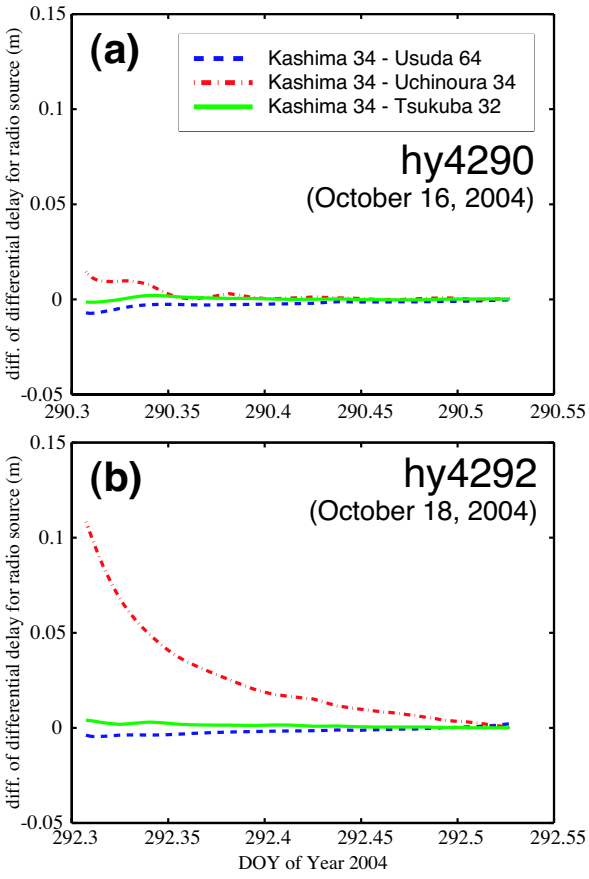

Figure 6. Upper: Difference between the differential delays during the first experiment hy4290; Lower: Same plot but for the second experiment hy4292.

zero. It suggests that the difference procedure is efficient to correct the errors due to the atmospheric path delay under calm weather conditions. On the other hand, the characteristics of the time series for the Kashima-Uchinoura baseline as shown upper and lower panels are very different each other. The maximum value of differences is less than 1.5 cm over the first experiment period (upper panel), whereas the maximum value of differences is up to more than 10 cm during the second experiment period (lower panel).

The primary cause of the large difference value is a significant difference in water vapor content during the second experiment at Uchinoura and Kashima. We can infer from a experiment schedule and a baseline azimuth that the effect is emphasized by the difference in elevation angle of radio source at both stations. Since the baseline vector between both stations is toward the west and the radio sources were in the southeastward direction, about four degrees in the elevation angle at Uchinoura is smaller by comparing with that at Kashima at the beginning of the second experiment period.

In general, we can estimate an atmospheric path delay as the one of unknown parameters from the VLBI observables only. However, it is essentially difficult to perform the same way in the $\Delta VLBI$ measurement analysis. Because the elevation and azimuth angles of the radio sources are not homogeneously distributed in the sky, a least square estimation becomes unstable due to the mutual distinguishability among the parameters.

In this report we mention about to use the GPS-based ZWD estimates to evaluate the effects of atmospheric correction on the $\Delta VLBI$ measurements. At present, these estimates for each station have enough precision to improve the numerical weather prediction (NWP) models[7], [8]. The recent studies indicate that the GPS-based ZWD estimates agree well with those obtained by radiosonde data sets or a water vapor radiometer (WVR) at a few millimeter rms level(ex. [10], [11]). Therefore, we are going to develop a new correction method based on the estimates in order to remove the atmospheric path delay error from the VLBI observables.

6. Summary

We performed two $\Delta VLBI$ experiments for the HAYABUSA spacecraft on October 16th and 18th, 2004. In these experiments we acquired the geodetic GPS data sets from the IGS stations and one

GEONET GPS station of the GSI, Japan. These GPS stations are adjacent to the each VLBI station participated the experiments. We evaluate an effect of cancelling out atmospheric path delay errors on the $\Delta VLBI$ measurements based on the delays derived from geodetic GPS analysis. According to our analysis, a large difference value of up to 10 cm of the differential path delay for the Kashima-Uchinoura baseline was estimated in spite of a small separation angle of less than 3 degrees between the HAYABUSA spacecraft and quasar. Such large value was mainly caused by the humid condition around Uchinoura due to the typhoon approaching. Moreover, the east-west direction of the baseline vector and the large difference in elevation angle of radio source between both stations helped to enlarge the difference value.

References

[1] *www.igs.nasa.gov*

[2] *cddis.gsfc.nasa.gov/ftpgpsstruct.html*

[3] *igscb.jpl.nasa.gov/components/data.html*

[4] Rothacher. M., Orbits of Satellite Systems in Space Geodesy. *Geodaetisch.geophysikalische Arbeiten in der Schweiz*, 46, 1992.

[5] Davis et al., Geodesy by radio interferometry: effects of atmospheric modeling errors on estimates of baseline length, *Radio Science*, **Vol. 20**, No. 6, pp. 1593-1607, 1985.

[6] Niell, A., Global mapping functions for the atmosphere delay at radio wavelength, *J. Geophys. Res.*, **101(B2)**, 3227-3246, 1996.

[7] Reigber et al., Near real-time water vapor monitoring for weather forecast, *GPS World*, **13**, 18-27, 2002.

[8] Gendt G et al., Near real time GPS water vapor monitoring for numerical weather prediction in Germany. *J. Meteor. Soc. Japan*, **82(1B)**, 361-370, 2004.

[9] *www.jma.go.jp*

[10] Behrend et al., An inter-comparison study to estimate zenith wet delays using VLBI, GPS, and NWP models, *Earth Planets Space*, 52, 691-694, 2000.

[11] Haefele et al., Impact of radiometric water vapor measurements on troposphere and height estimates by GPS, *Proceedings of the 17th International Technical Meeting of the Satellite Division of The Institute of Navigation (ION GNSS 2004)*, Sept. 21-24, 2004.

Phase Calibration Signal Generator

–preliminary evaluation –

Mamoru Sekido (sekido@nict.go.jp), Hiromitsu Kuboki, and Eiji Kawai

Kashima Space Research Center, National Institute of Information and Communications Technology 893-1 Hirai, Kashima, Ibaraki 314-8501, Japan

Abstract

Phase calibration signal generators (PCAL antenna unit) were developed for future replacement with the current PCAL antenna unit on 34m antenna at Kashima. Group delay characteristic with the new PCAL units were evaluated and it was confirmed as the same level with the current one. Cable delay measurement function is not implemented in the new PCAL unit at present yet, but the 'delay cal' function will be considered in near future.

1. Introduction

Phase calibration (PCAL) antenna unit is an important equipment for geodetic VLBI observation. A basic block diagram of VLBI receiver system is shown in Figure 1. Phase calibration signal is composed of a set of tone signals with 1 MHz interval. Since phases of every tone signals are aligned at the injection point, total phase shift due to the signal transmission delay from the top of the receiver system till to the sampling point and initial phase of local oscillators in video converters is observed in PCAL phase at the sampling point. This phase of PCAL signal observed at the sampler is used for calibration of phase delay variation caused in the signal line from the top of the receiver system to the sampler. And it is very necessary for the bandwidth synthesis procedure [1] to obtain high precision group delay in VLBI observation. A PCAL-antenna-unit of K-3 VLBI system[2][3][4][5] has been used in the 34m antenna at Kashima. Because about 20 years have passed since its designing, some microwave components of the PCAL-antenna-unit, such as step recovery diode (SRD) and microwave switch, are no more available now. A trouble of breaking down of microwave switch in the PCAL-antenna-unit had happened in 2003. Fortunately we could repair it by replacing with another microwave switch at that time. Although if SRD is broken, the same type of SRD driven by 10 MHz signal is no more available now. Also we could not find any companies providing PCAL system at that time. Then we decided to search for alternative SRD device and microwave switches. And we ordered two companies to produce P-CAL generator for future replacement with the K-3 PCAL-antenna-unit.

2. PCAL generator

A SRD chip driven by 10 MHz signal was available from Aeloflex metelics company [6]. Although it need to be assembled to a microwave component by adding impedance matching circuit. Then we have chosen another SRD product (GCA100A) provided by Herotek Inc.[7]. Advantages of that SRD are that pre-amplifier is integrated in it and it can output comb tone signal up to 50 GHz. A drawback of the SRD is, however, that it need to be driven by 100 MHz reference input signal instead of 10 MHz. To keep the compatibility of 10MHz reference input with the current PCAL-antenna-unit, 100 MHz output phase-locked oscillator (HPLL-100M-S) provided by DST technology Inc.[8] was introduced as the source of 100 MHz signal. High speed microwave switch (CMCS-0337) [9], whose typical transition time is 2 ns, was used for gating the comb pulses in time domain. We ordered two companies (Digital Link Inc. and Cosmo Research Co. Ltd.[10]) to assemble the components to for PCAL-antenna-unit. Designing of logic circuits for counting 100 MHz signal to control the microwave switch for gating the pulse train in time domain were made by each companies. Pictures of the PCAL-antenna-units are displayed in figure 2.

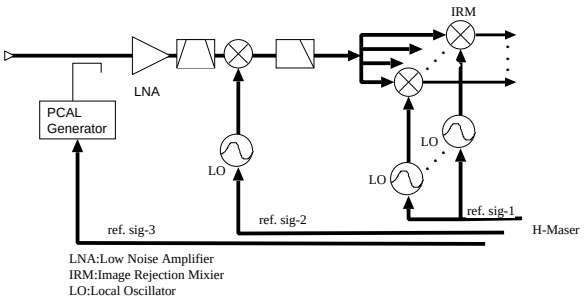

Figure 1. A basic block diagram of receiver system of geodetic VLBI. Local oscillators of the receiver system is locked with phase of reference signal generated by hydrogen maser. And Radio frequency signal received at the Antenna is down converted to multiple video channels. Multiple tone signal generated by PCAL-antenna-unit are injected from top of the receiver system.

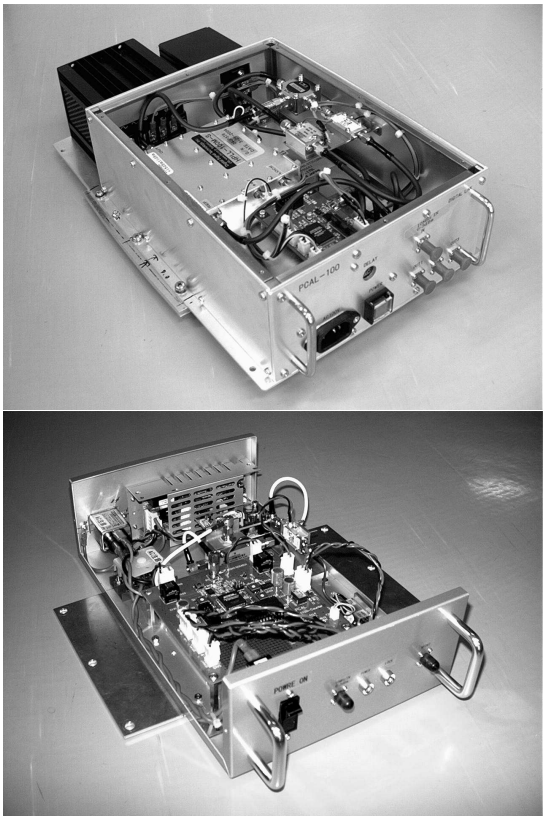

Figure 2. PCAL-antenna-unit produced by Digital Link Inc. (Upper) and Cosmo Research Co. Ltd. (Lower), respectively.

3. Preliminary comparison of the PCAL-antenna-units

Group delay characteristics of the newly produced PCAL-antenna-units and the K-3 type PCAL unit are compared. Amplitude and phase of 8 channel of PCAL signal each in X-band and S-band were measured every two minutes by using a PCAL detection function of the K-4 VLBI sampler (K-4 Input Interface) [2]. The local frequency setup table of video converter is shown in Table 1. The K-3 type PCAL-antenna-unit, which was produced by Meisei electric Co. Ltd., is indicated as M-pcal. Newly assembled PCAL-antenna-units are indicated as D-pcal (Digital Link Inc.) and C-pcal (Cosmo Research Co. Ltd.). Strength of the PCAL tone signal was fairly flat over the receiving frequency range both in X-band and S-band. Amplitude of of PCAL signal detected with the K-4 input interface was in the range from 2 to 10 % for all channels. Unfortunately the comparison of PCAL system was not made in perfect condition in this report, because all the PCAL-antenna-units are not compared with the same frequency set up (Table 1). Even though, we could see that the group delay characteristic of the three types of PCAL-antenna-

Table 1. Frequency table of video converter local frequency setup. Table (1) was used for the M-pcal and the C-pcal, and table (2) was used for the D-pcal. Ambiguity of group delay is reciprocal of GCM (Greatest common measure) and delay resolution is proportional to the inverse of EBW (effective bandwidth).

Channel	(1)		(2)	
	X-band	S-band	X-band	S-band
1	629.99	719.99	629.99	676.99
2	639.99	724.99	639.99	686.99
3	669.99	739.99	669.99	712.99
4	729.99	769.99	729.99	800.99
5	839.99	799.99	810.99	830.99
6	919.99	809.99	830.99	835.99
7	969.99	824.99	840.99	840.99
8	989.99	834.99	850.99	843.99
GCM (MHz)	10	5	1	1
EBW (MHz)	396.59	121.02	249.12	194.24

units are in almost the same level. Hereafter we call the delay obtained by the synthesized delay resolution function as *pseudo group delay*. Figure 3 shows behaviour of the pseudo group delay obtained by synthesizing 8 channels of complex number of PCAL data for each X-band and S-band. Initial phases of each channels of PCAL data are subtracted as a reference, thus every plots of the pseudo group delay start from zero. We could see that variations of pseudo group delay are approximately about 1 ns while 1.5 days in any cases of PCAL-antenna-units. Since we have newly employed a 100 MHz PLO system in the new PCAL system, phase drift due to daily temperature variation at antenna receiver room was concerned. Room temperature at the receiver room and surface on the PCAL-antenna-unit were monitored simultaneously at the time of the measurements. However, we could not see any evidence of the temperature effect. If the variation of pseudo group delay is caused by the phase variation of reference signal (10MHz or 100MHz), magnitude of the variation in X-band must be 4 time larger than S-band. Although actual data shows that the variation in S-band is much larger than that in X-and. We don't have definite interpretation of this behaviour at present. But it seems to attributed to the characteristic of the receiver system itself, since the same phenomenon is observed in all three different sets of PCAL-units. Since this comparison test result include the influence of receiver system and reference signal distribution from hydrogen maser to the antenna receiver, we are planning to test the PCAL system with Giga-bit sampler, which will enable direct measurement of wide band characteristic of PCAL signal. Current PCAL system does not work with *delay calibration system*, which monitors the variation of

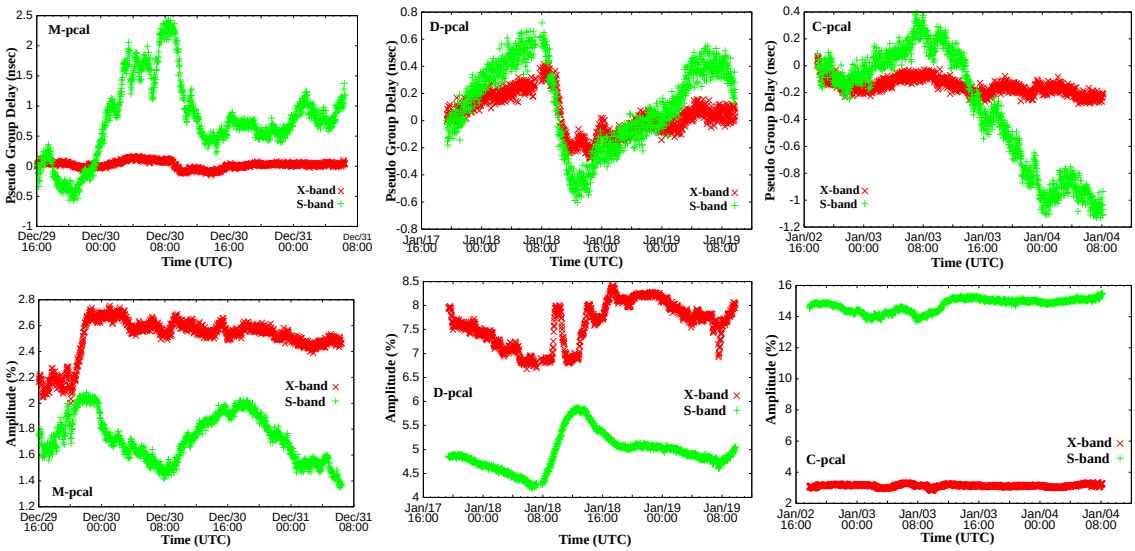

Figure 3. Pseudo group delay (upper panel) and synthesized amplitude (lower panel) of PCAL signal. Each plots indicate M-pcal (Meisei electric Co. Ltd.), D-pcal (Digital Link Ltd.), and C-pcal (Cosmo Research Co. Ltd.) from the left to the right. The symbol of '+' and '×' in the plots are data of S-band and X-band, respectively.

reference signal transmission delay from hydrogen maser to the PCAL reference input. This is also important component for geodetic VLBI observation, but its function was eliminated in this P-CAL unit. It was because the effect of 'cable delay' was estimated together with atmospheric parameter in the old analysis strategy at Kashima. We are thinking to implement delay calibration function in the new PCAL system.

4. Summary

Preliminary evaluation of newly assembled PCAL-antenna-unit are described. Pseudo group delay behaviour was almost the same for the old K-3 type PCAL and new ones. Larger pseudo group delay variation in S-band than that of X-band was observed for all cases of the PCAL units. It might be attributed to the S-band receiver system. Further check of the receiver system may be required. Delay calibration function will be considered in the next version.

References

[1] Alan E. E. Rogers, "Very long baseline interferometry with large effective bandwidth for phase-delay measurements", Radio Sci. Vol.5, No.10 pp.1239-1247, 1970.

[2] Kiuchi H., S.Hama, J. Amagai, Y. Abe, Y. Sugimoto, and N. Kawaguchi, "III.2 K-3 and K-4 VLBI Data Acquisition Terminals", J. Comm. Res. Lab., Vol. 38, No.3, pp. 435-457, 1991.

[3] Hama S., and H. Kiuchi, "III.3 K-3 and K-4 VLBI Data Recorders", J. Comm. Res. Lab., Vol. 38, No.3, pp. 459-470, 1991.

[4] Sugimoto Y., S. Hama, and H. Kiuchi, "III.4 K-3 and K-4 VLBI Data Correlation Processors", J. Comm. Res. Lab., Vol. 38, No.3, pp. 471-480, 1991.

[5] Takahashi Y., S. Hama, and T. Kondo, "III.5 K-3 Software System for VLBI and New Correlation Processing Software for K-4 Recording System", J. Comm. Res. Lab., Vol. 38, No.3, pp. 481-501, 1991.

[6] Aeroflex Metelics *http://www.metelics.com/pi1.htm*

[7] Herotek Inc. *http://www.herotek.com/datasheets/protoc.html#GENERATOR*

[8] DST Technology *http://www.dst.co.jp/en/*

[9] Custom Microwave Components Inc. *http://www.customwave.com/home.html*

[10] Cosmo Research *http://www.cosmoresearch.co.jp/index.html*

On the expansion of the frequency coverage of an X-band of Kashima 34-m antenna

Eiji Kawai (*kawa@nict.go.jp*),
Hiromitsu Kuboki, Yasuhiro Koyama, and Tetsuro Kondo

Kashima Space Research Center,
National Institute of Information and Communications Technology
893-1 Hirai, Kashima, Ibaraki 314-8501, Japan

1. Introduction

Nominal frequency coverage of an X-band of Kashima 34-m antenna is from 7860 MHz to 8600 MHz. This frequency coverage was determined on the basis of a geodetic VLBI conducted about more than 10 years ago. Recently the demand to receive wider frequency coverage arises for an international VLBI experiment to increase the accuracy of measurements. Actually some sessions under the IVS have already conducted using a new frequency allocation of which an upper frequency in the X-band is expanded to higher frequency up to 9080MHz exceeding the upper limit of the current X-band receiving system of Kashima 34-m antenna. In order to expand the nominal frequency coverage of Kashima 34-m antenna, we have checked the performance of X-band receiving system by replacing a bandpass filter in the down converter unit which limits the highest frequency in the X-band receiving system.

2. Frequency characteristics of T_{sys} and SEFD

An X-band receiving system of Kashima 34-m antenna consists of three receivers, which are named X-n (X-narrow), X-wH (X-wide High), and X-wL (X-wide Low), respectively. X-wH and X-wL share a common LNA (low noise amplifier) and receive the same circular polarization component, while X-n receives the circular polarization component opposite to that of X-wH and X-wL. For an example, when X-wH and X-wL receive the right-handed circular polarization, X-n receives the left-handed one, and vice versa. Current frequency coverage of each receiver is summarized in Table 1. Figure 1 shows a measurement block diagram. We have measured the frequency characteristics of system temperature (T_{sys}) and system equivalent flux density (SEFD) for the X-n receiver from 8180 MHz up to 9080 MHz by replacing a bandpass filter (BPF), which is inserted between the LNA and a mixing circuit, according to a frequency to be measured, i.e., an 8180-8600MHz BPF is used for measurements below 8600 MHz while an 8580-9080MHz BPF is used for 8600 MHz and higher.

Table 1. Frequency coverage of X-band receivers.

Receiver	Frequency Coverage (MHz)
X-n	8180-8600
X-wL	7860-8360
X-wH	8180-8600

When nominal frequency range, 8180 - 8600 MHz, is received, the intermediate frequency (IF: 100 - 520 MHz) is further up-converted to match with the input frequency range (500 - 1000 MHz) of the KSP-type K4 video converter (K4VC). The IF output is connected directly with K4VC in thecase of higher frequency 8580 - 9080 MHz reception. Video signal output of 2 MHz band width is measured by using the power meter (hp 438A) combined with a power sensor (hp 8484A). Measurement was performed on June 14, 2005 for about 4 hours. Temperature, humidity, and pressure on that date were 18 °C, 80 %, and 1009 hPa, respectively. T_{sys} was measured by using a Y-factor method. Let the ratio of the video output (P_{cold}) when cold load is connected to the receiver and video output (P_{sky}) when the antenna pointed to no radio source region in the sky is connected be Y1 ($=P_{cold}/P_{sky}$), and the ratio of the video output (P_{hot}) when hot load is connected and P_{sky} be Y2 ($=P_{hot}/P_{sky}$). T_{sys} is given by:

$$T_{sys} = \frac{T_H - T_C}{Y2 - Y1} \tag{5}$$

where T_H is physical temperature of hot load, and T_C is physical temperature of cold load.

Measured T_{sys} is shown in Figure 2 (upper panel). T_{sys} at frequency range 8180 - 8600 MHz shows almost flat characteristics and their average was 53K. T_{sys} at higher frequency range 8600 - 8850 MHz shows also almost same characteristics as seen in the lower frequency band. However T_{sys} increases with frequency when it exceeds 8900 MHz. The diplexer which is placed at the input of the IF amplifier causes this T_{sys} increase as described later. SEFD was obtained on the basis of the measurement of Virgo-A (46 Jy at 8 GHz) by using a following equation.

$$SEFD = \frac{S}{(P_{on} - P_{off}) - 1} \tag{6}$$

where S is flux density in Janskys, P_{on} is receiver output power of "on" source, P_{off} is receiver output power of "off" source.

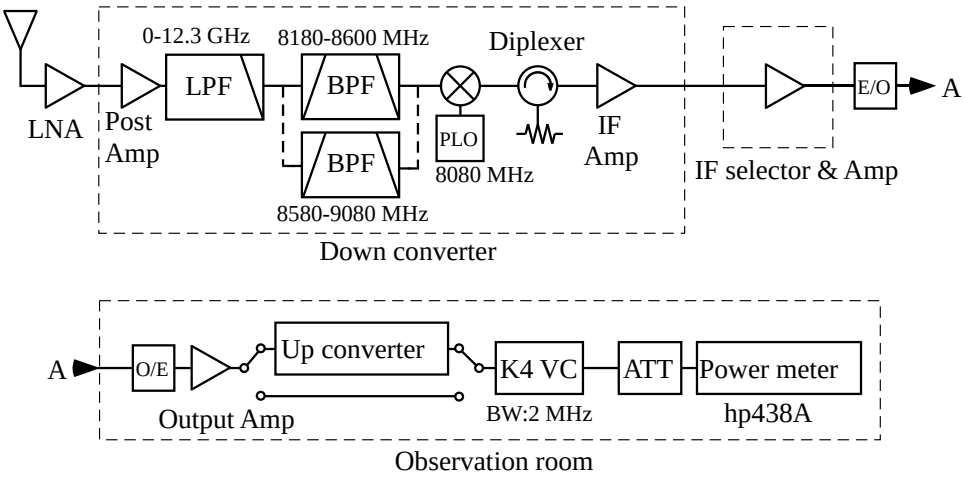

Figure 1. A block diagram of the performance measurement of X-band receiving system.

Measured SEFD is shown in Figure 2 (middle panel). The elevation angle of the antenna changed from 64 degrees (during the measurements for lower frequency range) to 52 degrees (for the higher frequency range). However an elevation dependency is not corrected here. Measured SEFD was about 232 Jy at lower frequency range. At higher frequency range (8580 - 8850 MHz), SEFD was measured as about 237 Jy and it is almost same as lower frequency's. P_{hot} is also plotted in the lower panel of Figure 2. As shown in the figure, P_{hot} decreases when frequency increases and approaches almost zero at $>$ 8900 MHz. Rapid increase of T_{sys} and SEFD at higher frequency region ($>$ 8900 MHz) is thought to be reflected these uncertain measurements of P_{hot}. Considering LNA (from 8 GHz up to 9 GHz), IF selector and amplifier (up to 1 GHz), optical transmitter E/O (up to 5 GHz), optical receiver O/E (up to 3 GHz), and output amplifier after O/E (up to 2 GHz) have sufficient bandwidth coverage, it is suspected that a post amplifier after LNA, IF amplifier after mixer, and diplexer after IF amplifier may not have sufficient band width coverage.

We have therefore measured frequency characteristics of these components and found that the frequency characteristics of the diplexer is insufficient as shown in Figure 3. The gain of the post amplifier is about 20 dB and shows almost flat characteristics at frequencies from 8180 MHz up to 9080 MHz. The gain of the IF amplifier decreases by about 2 dB at 861 MHz which is equivalent to 8941 MHz in sky frequency which is required by frequecy expanded experiments. The diplexer shows low-pass filter characteristics with a cut-off frequency of 750 MHz corresponding to 8830 MHz in sky frequency. The attenuation at 861 MHz corresponding to 8941 MHz insky frequency is about 10 dB. Hence

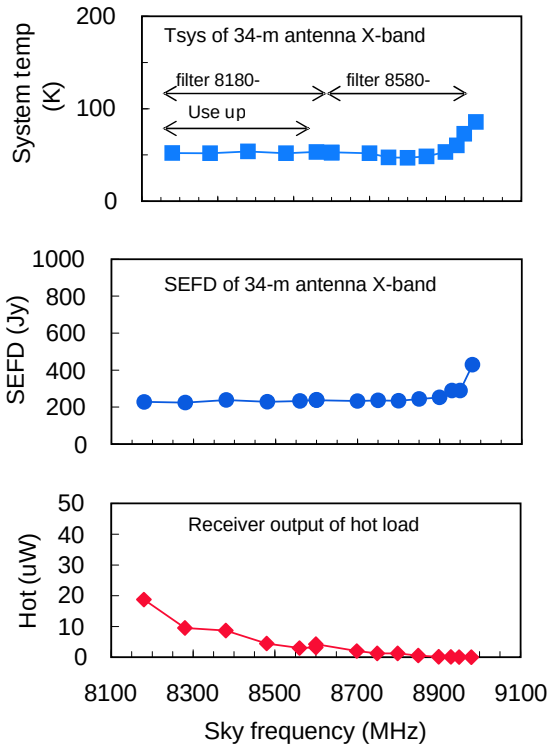

Figure 2. Tsys (upper panel), SEFD (middle panel), and video output of hot load (lower panel) of X-band wider band.

the major reason for rapid increase seen in T_{sys} and SEFD at a higher frequency region can be attributed to the insufficient frequency coverage of the diplexer. If we remove the diplexer, the power loss in the down converter output is expected to become merely 2 dB at 8941 MHz. After the annual maintenance of the 34-m antenna, we will check the frequency characteristics of T_{sys} and SEFD again

without the diplexer.

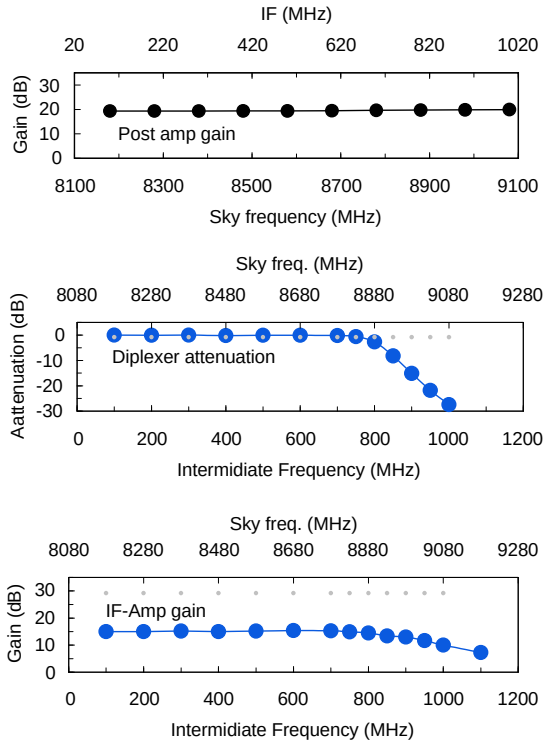

Figure 3. The frequency characteristics of post amplifier (upper panel), diplexer (middle panel) and IF amplifier (lower panel).

3. Conclusions

The frequency characteristics of the 34-m antenna X-band receiver has been measured by replacing the band-pass filter. It has been found that T_{sys} and SEFD at a frequency range 8580 - 8850 MHz show the almost same characteristics as those measured at a nominal frequency range 8180 - 8600 MHz. At a higher frequency range (8580 - 9080 MHz), T_{sys} and SEFD however increase rapidly when the frequency exceeds 8900MHz. The major reason of this rapid increase is considered to be attributed to an insufficient bandwidth of the diplexer placed at the input stage of the IF amplifier. We will check T_{sys} and SEFD without the diplexer to extend the bandwidth of the 34-m X-band receiver.

Development of the software correlator for the VERA system

Moritaka Kimura (*mkimura@nict.go.jp*)

Kashima Space Research Center,
National Institute of Information and Communications Technology
893-1 Hirai, Kashima, Ibaraki 314-8501, Japan

1. Introduction

VERA (VLBI Exploration of Radio Astrometry) is the modern Japanese VLBI system for astronomy. Main target of this system is dedicated to differential VLBI to measure the position and proper motion of the galactic masers with 10 micro arcsec level accuracy. Almost all equipments such as radio telescopes, magnetic recorders, digital filter and etc, were developed newly, however the VSOP-FX correlator developed in the VSOP project was reused for VERA system. This correlator was designed around 1990 and maintenance will be more difficult forward, however the VERA project is started from 2000 and it will be continued at least 15 years. A new correlation system is required for stable operation of the VERA project. There is another serious problem in addition to maintenance as long as using the VSOP-FX correlator. The number of radio telescope which can be processed simultaneously by the VSOP-FX was halved in only five for adaptation to VERA system. Number of the radio telescopes which can join with the VERA will be increase in Japan. It is possible to replace the hardware correlator by software correlator, because the data rate of the VERA system is only 1Gbps [1]. There is no limit of the number of radio telescopes for software correlator, and it can construct very cheaply. The software correlator developed by NICT was determined as a next correlator of the VERA system.

2. System Configuration

Many data communications parts of the VERA system are designed by the VSI-H standard except magnetic recorders and the hardware correlator. The block diagram of the VERA system with software correlator is shown in Figure 1. Most observations of the VERA project are differential VLBI using two beams, two A/D samplers are prepared for each station. Two VSI-H signals from two A/D samplers are split into several channels by digital filer and merged into one VSI-H signal. This VSI-H signal is converted into VERA original data format

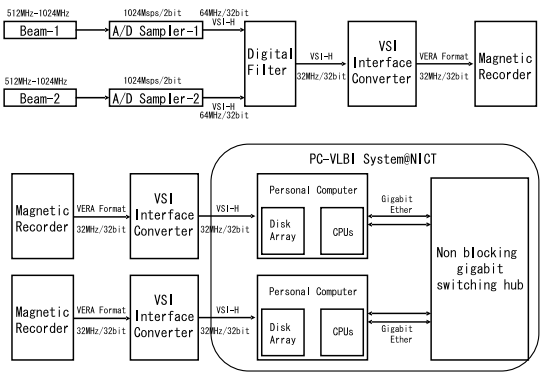

Figure 1. The VERA system with the software correlator.

to recording on magnetic tape. After observation has finished, magnetic tapes were sent to the correlation center and play backed data is recorded on the disk array again. The software correlator installed in each PCs perform correlation processing using the data recorded on the disk array. If the fastest PC is used for correlator, correlation processing of four telescopes can be performed on near real time by one PC, In the viewpoint of processing speed. However, it is difficult to import four 1-Gbps data to one PC continuously. Since the number of observation stations of VERA is four, four sets of PCs are used. Even, if more radio telescopes join, simultaneous correlation processing of all the baselines is possible by preparing PCs of the same number. [2].

3. Connection between the VERA system and the NICT system

The system developed by NICT was carried to the National Astronomical Observatory Mitaka correlator center and the first joint experiment was performed on August 2, 2005. Although each equipments developed in the independent institution, the signal played back from the magnetic recorder was recorded on the disk array without any trouble. The data used this experiment was recored by typical VERA observation mode and there are 16 channels each channel have 16MHz band width. The software correlator program could process this mode without any editing, because this recording mode is the completely same data format as the data that were recorded using ADS2000 sampler which has 16 analog A/D channels developed by NICT. The first fringe of 3C273B between Mizusawa and Ogasawara telescopes processed by the software correlator is shown Figure 2. Results of

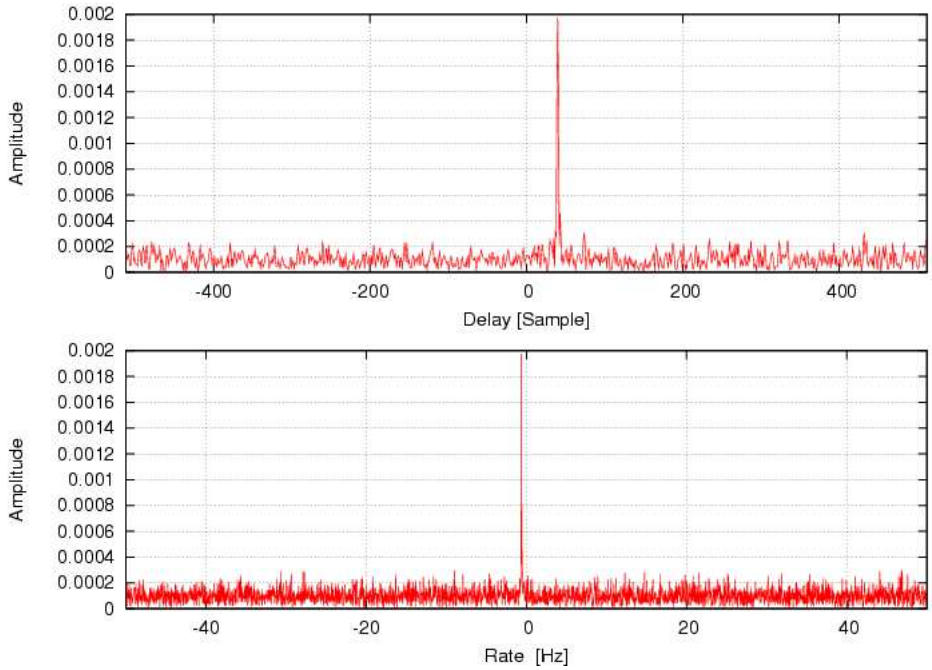

Figure 2. The first fringe of the VERA observation processed by the software correlator.

hardware and software correlation showed good coincidence.

4. Future plan

The purpose of this experiment is checking the electric connection between the VERA system and the NICT system, and it was confirmed that it is satisfactory. It is the stage which still succeeded in fringe detection at present. Development of the full-scale system which can perform automatic operation as the VERA correlation system will complete in about one year.

References

[1] Kimura, M., J. Nakajima, T. Kondo and H. Takeuchi. (2003), 2-Gbps PC architecture and Gbps data processing in K5/PC-VSI. IVS CRL-TDC News, No. 23, pp. 12-13.

[2] Kimura, M. and J. Nakajima. (2002), The implementation of the PC based Giga bit VLBI system. IVS CRL-TDC News, No. 21, pp. 31-33.

A multi-stream FFT library for VLBI

Hiroshi Takeuchi (*ht@nict.go.jp*)

Kashima Space Research Center
Institute of Information and Communications Technology, 893-1 Hirai, Kashima, Ibaraki 314-8501, Japan

Abstract: An FFT software library which is optimized for VLBI has developed. In the library, data from multiple different data streams (different baseband channels, different stations or temporally contiguous data sets in a single stream) are alternately stored in memory space and be processed simultaneously. It enables an efficient sequential access to the memory in the butterfly operations in the FFT algorithm. This library is written in x86 assembly language and SSE3 instruction set is used to accelerate its performance. To evaluate the performance of the library, we compared its performance against that of FFTW3 which is known as one of the fastest FFT libraries for many processors. As a result, it runs $20\% - 150\%$ faster than FFTW.

1. Introduction

Conventionally, digital-backend instruments in radio interferometer such as correlators or digital spectrometers are implemented with custom-built hardwares to process high-speed video band signals in real-time. In the mean time, performance of commodity PCs has increased so that we could use them in the digital-backend system of VLBI. In order to enhance the performance of such PC-based instruments, we developed an FFT library optimized for VLBI data streams.

2. Multi-stream FFT Library

In the FX-type software correlator, a large number of FFTs are repeatedly performed. If the multiple FFT operations can be integrated and be performed simaltaneously, there are following advantages: (1)Allowing effective data access to multi-channel data streams (see figure 1). (2)If N-sets of data streams are transformed simultaneously, the number of data transfers to load FFT twiddle factors to CPU's registers becomes 1/N. (3)While the bit-reverse permutation at the last stage of FFT is nearly random access across the memory in the case of normal FFT libraries, N-sequential memory access can be used in the multi-stream FFT. (4)If each input stream of the multi-stream FFT is allocated to stream from different station, same frequency channels from different stations are adjoining in memory space after the FFT. As a result, 'X' part's operation in the FX correlator can be performed effectively without any redundant memory accesses.
Moreover, following VLBI-specific options can be easily implemented:

- Conversion from the input raw-data streams to the FFT-input floating-point vectors can be easily included in the first stage of FFT.
- Fringe rotation can be included in butterfly operations in the first stage of FFT. Trigonometric functions table for the rotation can be shared with the FFT twiddle factor table.
- If each input stream is corresponding to different baseband channels in a single station, fractional-bit compensations after FFT can be neglected by using phase-shifted FFT twiddle factors.

On the other hand, required buffer size for N-stream parallel FFTs is N times greater than that for normal FFT. If the required buffer size exceeds L2-cache size of the system, performance of the library will be degraded significantly. By using SSE registers of x86 processor, four floating-point values can be operated simultaneously. In the present FFT library, two complex values from two independent data-sets are loaded from memory to a SSE register with a single instruction, and simultaneously calculated with SSE instructions.

- Environment: Intel Xeon 3.40 GHz, L1 cashe:8KB,L2 cache:1024KB,Main memory 4GB,Using a single CPU (IA32).
- Test data length: 10G samples $\times$ 5 times (error bar in the graph is based on the standard deviations of five results)
- FFTW 3.0.1: real-to-halfcomplex conversion, single-precision, compiled with GCC -O3, using SSE functions, FFTW_EXHAUSTIVE option is used.
- Multi-stream FFT library: 8-streams of parallel operation, real-to-halfcomplex conversion, single-precision, written in assembly language (nasm), using SSE and SSE3 functions, Cooley-Tukey, radix-4, out-of-place(dual buffer).

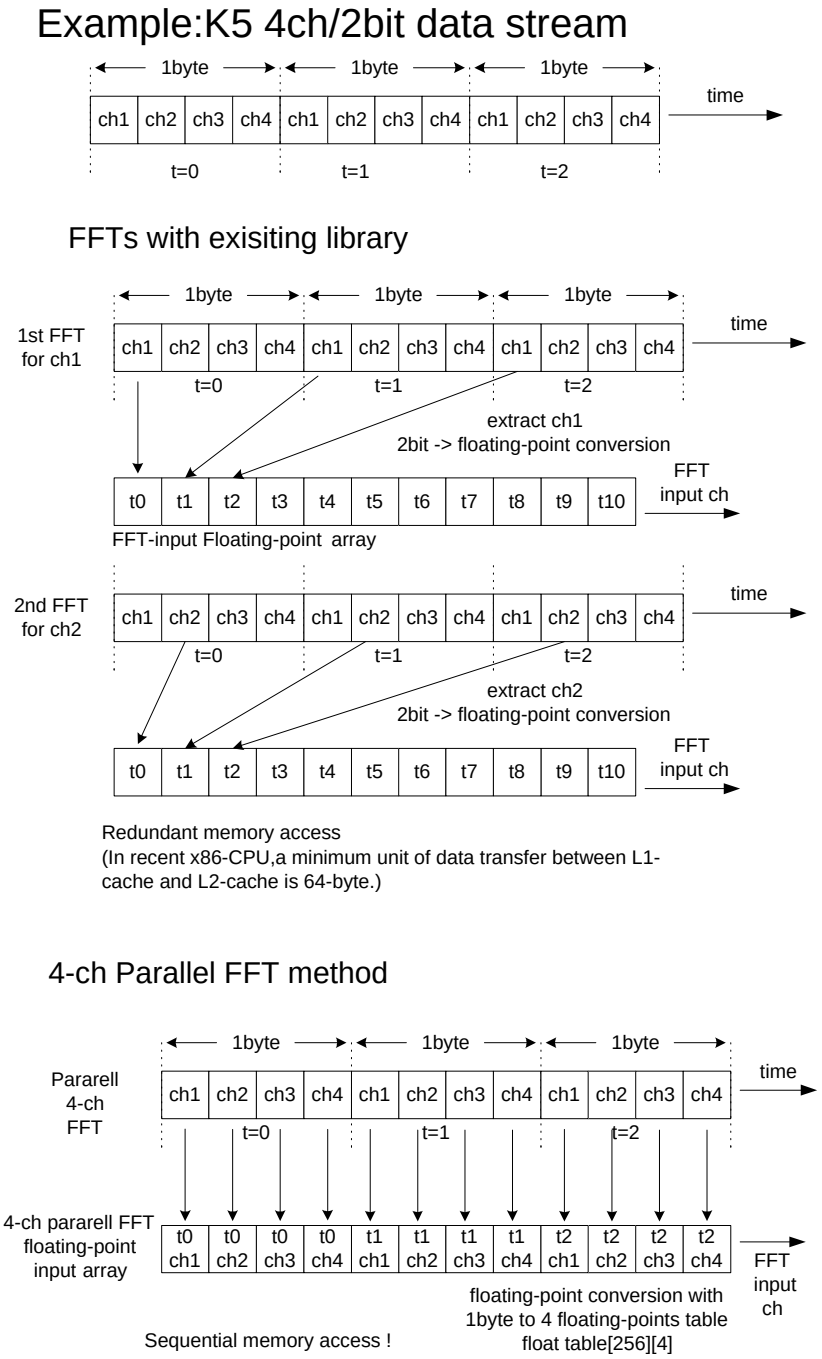

Figure 1. Data flow comparison between the multi-stream FFT library and the existing library.

3. Benchmark

Numerical experiments were carried out to evaluate the performance of the newly developed library. As shown in figure 2, the library's performance were compared with that of FFTW3. Benchmark conditions are as follows:

For eight streams of N-point real FFTs, the library needs $8 \times (\frac{N}{2} + 1) \times 2(\text{real/imaginary}) \times 2(\text{dual buffer}) \times 4(\text{size of float})$ bytes of data buffers and $\frac{3}{4}N \times 2(\text{real/imaginary}) \times 4(\text{size of float})$ bytes of FFT twiddle factor table. Figure 2 shows that new library has faster performance than FFTW if the required buffer size is less than the size of L2-cashe memory of the system.

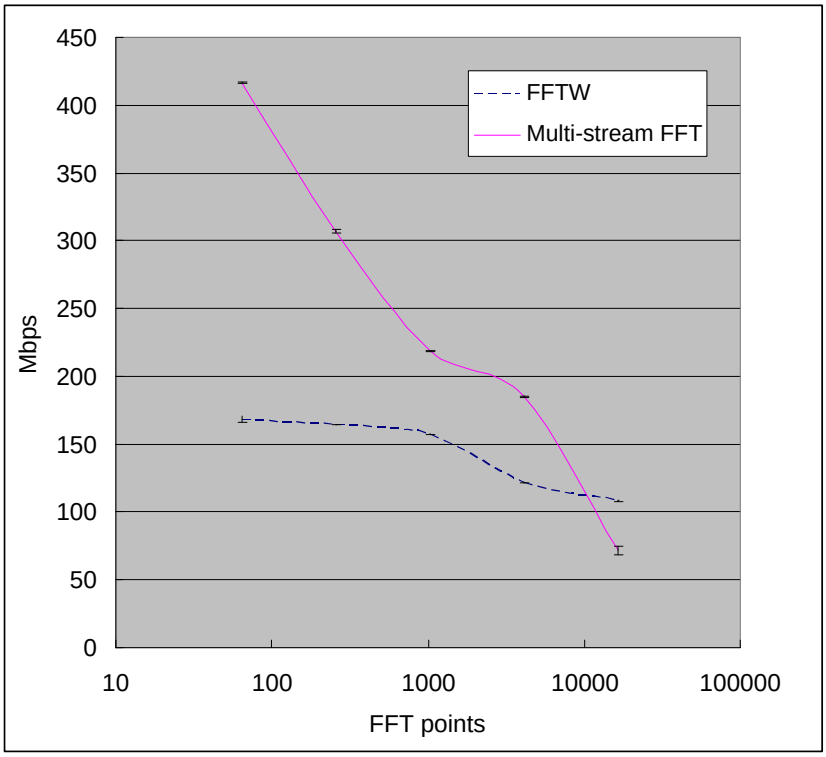

Figure 2. Benchmark results between the multi-stream FFT library and FFTW3.

4. Conclusion

In order to boost PC-based VLBI instruments, a multi-stream FFT library has been developed. When the required buffer size is less than L2-cashe size of the host CPU, performance of the library reaches up to 250% of that of FFTW.
The library can be obtained from:
http://www.nict.go.jp/ka/radioastro/RandD/fft/
An FX-type correlator core library using this FFT library will also be available from this web page.

References

[1] M. Frigo and S. G. Johnson, FFTW: An adaptive software architecture for the FFT, Proc. ICASSP 1998 3, p. 1381

"IVS NICT Technology Development Center News" (IVS NICT-TDC News) published by the National Institute of Information and Communications Technology (NICT) (former the Communications Research Laboratory (CRL)) is the continuation of "IVS CRL Technology Development Center News" (IVS CRL-TDC News). (On April 1, 2004, Communications Research Laboratory (CRL) and Telecommunications Advancement Organization of JAPAN (TAO) were reorganized as "National Institute of Information and Communications Technology (NICT)".)

VLBI Technology Development Center (TDC) at NICT is supposed

1) to develop new observation techniques and new systems for advanced Earth's rotation observations by VLBI and other space techniques,
2) to promote research in Earth rotation using VLBI,
3) to distribute new VLBI technology,
4) to contribute the standardization of VLBI interface, and
5) to deploy the real-time VLBI technique.

The NICT TDC newsletter (IVS NICT-TDC News) is published biannually by NICT.

This news was edited by Tetsuro Kondo and Yasuhiro Koyama, Kashima Space Research Center, who are editorial staff members of TDC at the National Institute of Information and Communications Technology, Japan. Inquires on this issue should be addressed to T. Kondo, Kashima Space Research Center, National Institute of Information and Communications Technology, 893-1 Hirai, Kashima, Ibaraki 314-8501, Japan, TEL : +81-299-84-7137, FAX : +81-299-84-7159, e-mail : kondo@nict.go.jp.

Summaries of VLBI and related activities at the National Institute of Information and Communications Technology are on the Web. The URL to view the home page of the Radio Astronomy Applications Section of the Kashima Space Research Center is : **"http://www.nict.go.jp/ka/radioastro/"**.

IVS NICT TECHNOLOGY DEVELOPMENT CENTER NEWS No.26, September 2005

International VLBI Service for Geodesy and Astrometry
NICT Technology Development Center News
published by
National Institute of Information and Communications Technology, 4-2-1 Nukui-kita, Koganei, Tokyo 184-8795, Japan